

1
2 **Topographic Heterogeneity and Aspect Moderate Exposure to Climate**
3 **Change Across an Alpine Tundra Hillslope**
4

5 **K. R. Jay¹, W. R. Wieder^{1,2}, S. C. Swenson², J. F. Knowles³, S. Elmendorf^{1,4}, H. Holland-**
6 **Moritz⁵, K. N. Suding^{1,4}**

7 ¹Institute of Arctic and Alpine Research, University of Colorado, 4001 Discovery Dr, Boulder,
8 CO 80303, USA.

9 ²National Center for Atmospheric Research, 1850 Table Mesa Dr, Boulder, CO 80305, USA

10 ³Department of Earth and Environmental Sciences, California State University, 400 W. First St,
11 Chico, CA 95929, USA.

12 ⁴Department of Ecology and Evolutionary Biology, University of Colorado, 1900 Pleasant St,
13 Boulder, CO 80302, USA.

14 ⁵Department of Natural Resources and the Environment, University of New Hampshire, 114
15 James Hall, 56 College Rd, Durham, NH 03824, USA.

16
17 Corresponding author: Katya Jay (katya.jay@colorado.edu)

18
19 **Key Points:**

- 20 ● Local abiotic heterogeneity (via differences in topography and aspect) governs snow
21 accumulation, runoff, and productivity in alpine tundra
- 22 ● Climate warming leads to earlier snowmelt, decreased runoff, and drier soils, potentially
23 decoupling plant resource demand and availability
- 24 ● Topographic position mediates exposure to climate change, highlighting potential
25 vulnerabilities of moisture-limited vegetation patches

Abstract

Alpine tundra ecosystems are highly vulnerable to climate warming but are governed by local-scale abiotic heterogeneity, which makes it difficult to predict tundra responses to environmental change. Although land models are typically implemented at global scales, they can be applied at local scales to address process-based ecological questions. In this study, we ran ecosystem-scale Community Land Model (CLM) simulations with a novel hillslope hydrology configuration to represent topographically heterogeneous alpine tundra vegetation across a moisture gradient at Niwot Ridge, Colorado, USA. We used local observations to evaluate our simulations and investigated the role of topography and aspect in mediating patterns of snow, productivity, soil moisture, and soil temperature, as well as the potential exposure to climate change across an alpine tundra hillslope. Overall, our simulations captured observed gradients in abiotic conditions and productivity among heterogeneous, hydrologically connected vegetation communities (moist, wet, and dry). We found that south facing aspects were characterized by reduced snowpack and drier and warmer soils in all communities. When we extended our simulations to the year 2100, we found that earlier snowmelt altered the timing of runoff, with cascading effects on soil moisture, productivity, and growing season length. However, these effects were not distributed equally across the tundra, highlighting potential vulnerabilities of alpine vegetation in dry, wind-scoured, and south facing areas. Overall, our results demonstrate how land model outputs can be applied to advance process-based understanding of climate change impacts on ecosystem function.

Plain Language Summary

It is critical to understand how rapidly warming mountain ecosystems will respond to environmental change. However, large differences in physical properties, including temperature,

snow, and water, over small distances make it difficult to project these responses. We used a land surface model that captures distributions of water and energy across the landscape paired with long-term observations from an alpine ecosystem to explore changes in snow, water, and productivity among diverse alpine vegetation. Additionally, we explored how this ecosystem might respond to climate change and how these responses differ across north and south facing slopes. Overall, our model results matched patterns in physical conditions and plant productivity observed at this site. We found that south facing slopes had less snow and drier, warmer soils compared to north facing slopes. Responses to climate change included snow melting earlier in the year, shifting the timing of runoff and suggesting that plant water demand may become disconnected from resource availability. Furthermore, responses differed across the landscape, indicating that plants in dry, wind-scoured, and south facing areas are more vulnerable to environmental change. Our study examines local-scale variation across an alpine landscape to address the challenge of projecting responses to change in rapidly warming ecosystems.

1 Introduction

Alpine and arctic tundra ecosystems are particularly sensitive to climate variability and change (Ernakovich et al., 2014; Seddon et al., 2016). Global air temperatures are rising, and high-elevation regions are warming faster than the rest of the planet; alpine records show an average rate of $0.3^{\circ}\text{C} \pm 0.3^{\circ}\text{C}/\text{decade}$ compared to $0.2^{\circ}\text{C} \pm 0.1^{\circ}\text{C}/\text{decade}$ globally (Hock et al., 2019). Mountain regions provide critical ecosystem services including supplying drinking water to half of the global population, but these water supplies are highly sensitive to climate change (Immerzeel et al. 2020). Moreover, warming in these high-elevation systems has potential implications for global carbon cycling via accelerated permafrost degradation (Knowles et al.,

2019), as has been shown in high-latitude permafrost systems (Schuur et al., 2015). Additional impacts of increasing temperatures in alpine systems include decreased snowpack (Musselman et al., 2021; Wieder et al., 2022), altered nutrient cycling (Dong et al., 2019), shifts in the timing of the growing season, and changes in vegetation composition (Walker et al., 2006). The exposure to these projected changes, however, may not be experienced evenly over alpine ecosystems.

Topographic gradients (formed by lateral drainage from hills to valleys) and aspect-driven differences in solar radiation represent primary controls on the availability of water and energy across landscapes, and thus the distribution of soil water and vegetation within ecosystems (Fan et al., 2019; Swenson et al., 2019). In mountainous terrain, topographic complexity at micro- and macro-scales (tens to thousands of meters, here referred to as ‘hillslope scales’; Swenson et al., 2019) drives variability in the accumulation and redistribution of snow and water – leading to gradients in soil conditions, hydrologic connectivity, nutrient cycling, and vegetation composition (Erickson et al., 2005; Opedal et al., 2015). Abiotic heterogeneity at hillslope scales can lead to microclimate differences where some parts of the landscape are buffered from atmospheric changes and act as refugia while other areas are more exposed, accentuating potential vulnerabilities (Lenoir et al., 2017; McLaughlin et al., 2017). Microscale variation can also mediate responses to climate warming (Körner & Hiltbrunner, 2021; Winkler et al., 2018; Zellweger et al., 2020), making it more difficult to predict how these systems will respond to change. Thus, exposure to climate change will likely be moderated by the heterogeneity generated by topographic complexity in mountain landscapes, where differences in topography and aspect alter abiotic conditions such as surface temperature, snow accumulation, and soil moisture. In the Colorado (CO) Rocky Mountains, slopes are predominantly north- and south-facing as a result of east-west draining valleys, leading to prominent variation in seasonal

snowpack depth and vegetation composition across aspects (Daubenmire, 1943; Helm, 1982; Hinckley et al., 2012). However, few studies have examined the role of topographic gradients and aspect in shaping patterns of snow, moisture, and productivity across alpine tundra landscapes and mediating their responses to climate warming.

At Niwot Ridge, CO, a Long-Term Ecological Research (LTER) site, a 70-year climate record shows that maximum annual temperatures have been increasing faster than the global rate at ~ 0.5 °C/decade (McGuire et al., 2012). Concurrent shifts in environmental conditions including precipitation and atmospheric deposition complicate efforts to understand alpine rates of response to warming. Indeed, previous studies have found conflicting responses that indicate alpine tundra ecosystems will both lag behind (Alexander et al., 2018; Körner & Hiltbrunner, 2021) and track (Panetta et al., 2018; Steinbauer et al., 2018) climate changes. Regional studies show that rising air temperatures have already led to earlier snowmelt and streamflow, as well as increases in the length of the ice-free period in alpine lakes (Christianson et al., 2021; Musselman et al., 2021). Heterogeneous terrain at Niwot Ridge leads to spatial variability in hydrologic connectivity, soil moisture, plant productivity, nitrogen (N) mineralization rates, and microbial biomass across the landscape (Chen et al., 2020; Hermes et al., 2020; Schmidt et al., 2015). Thus, we expect the effects of warming on nutrient cycling, productivity, and plant community composition to vary with topography and aspect.

To better understand how local heterogeneity mediates ecosystem responses to climate change, we used a land model with hillslope-scale processes to represent a heterogeneous alpine environment and examine ecological hypotheses. Land models simulate biophysical and biogeochemical processes, representing water, energy, carbon (C), and N fluxes (Lawrence et al., 2019). While these models are primarily used at global scales, they can be leveraged to address

ecologically relevant questions and provide insight into abiotic and biotic responses to climate change at regional and local scales (Mao et al., 2016). For example, Wieder et al. (2017) used the Community Land Model (CLM) version 4.5 to represent local patterns of water, energy, and C in alpine tundra, showing promise in exploring ecological responses to change. We build on this work using eddy covariance measurements from 2008-2021 at Niwot Ridge, CO to run single-point simulations of the CLM5 (Lawrence et al. 2019) with a hillslope hydrology configuration (Swenson et al. 2019) and site-specific modifications for moist, wet, and dry alpine vegetation (Figure 1). We first asked whether our modeling framework could reproduce observations of snow, soil temperature and moisture, and productivity across a topographically complex tundra hillslope (*Model evaluation*). We then applied this framework to examine how differences in solar radiation across north and south aspects alter patterns of hydrology, soil moisture and temperature, and growing season length (*Model application*). Finally, we extended our simulations to 2100 and examined whether microscale variation (via aspect and vegetation community) moderates exposure to climate change and ecosystem services (*Model projection*).

2 Methods

2.1 Study site

Our study was conducted at Niwot Ridge, a high-alpine LTER site in the Front Range of the CO Rocky Mountains, USA (40°03' N, 105°35' W, altitude approximately 3500 m above sea level, asl). Niwot Ridge has a mean annual temperature of -2.2°C and receives 884 mm of precipitation annually. Long term climate measurements from 1953–present at the D-1 site that hosts the highest elevation long-term weather station in North America at 3749 m asl show a strong warming trend at Niwot Ridge during the spring and summer months (Bueno de Mesquita

et al., 2021; McGuire et al., 2012). Precipitation patterns are highly variable and show a slight increase over time at alpine sites (Kittel et al., 2015). Indeed, high variability in total annual precipitation and mean monthly air temperatures seems characteristic of the site (Walker et al., 1994). Most of this precipitation (80%) falls as snow (Caine, 1996), leading to a short 2-3 month growing season. Niwot Ridge ecosystems range from subalpine forests to alpine tundra and talus. Our work here focuses on the dry, moist, and wet meadow vegetation that is broadly characteristic of alpine tundra ecosystems at the site.

Alpine tundra vegetation is structured largely by snow and its redistribution by wind across the topographically variable landscape (Erickson et al., 2005; Litaor et al., 2008), with some areas accumulating snow while other areas remain wind-scoured and snow free. Snow free areas, which host fellfield vegetation, and areas with thin snow cover, which host dry meadow vegetation, tend to be less productive and have low statured vegetation due to temperature and moisture adaptations (Billings & Mooney, 1968). In contrast, areas with deep snow accumulation host moist meadow communities, where snow persists into the summer and productivity is higher. Wet meadow vegetation forms in lowland areas that receive runoff from upland snowmelt and tend to have the highest productivity.

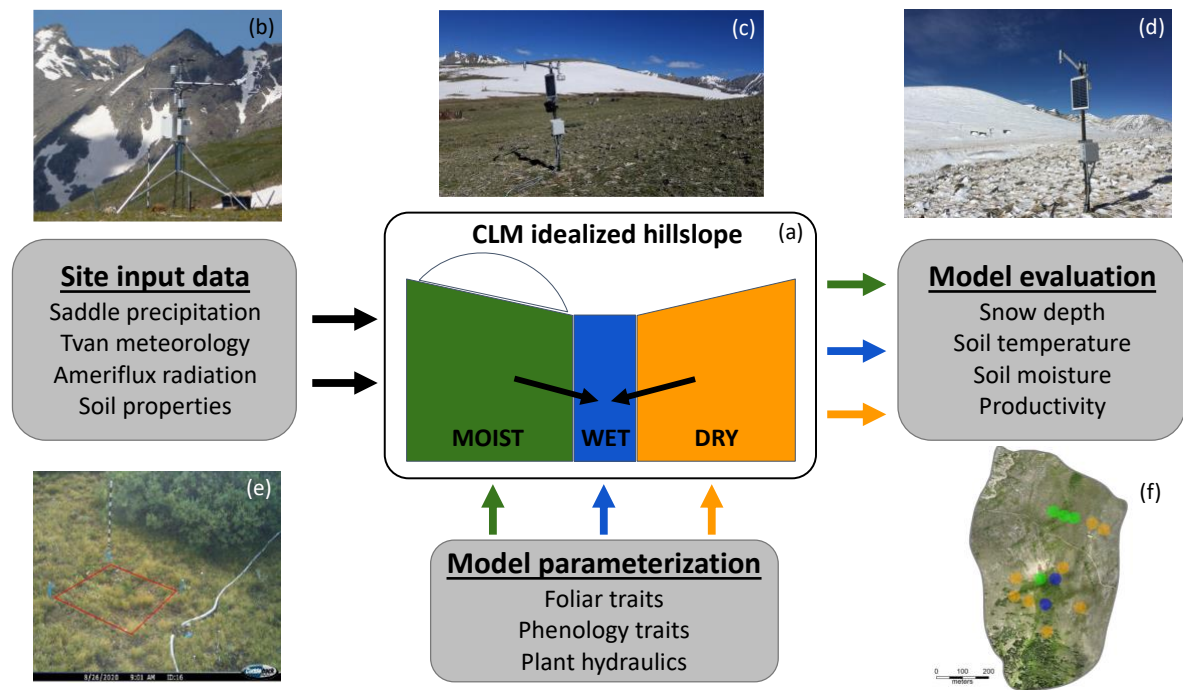
2.1.1 Site observations for model forcing and evaluation

Local meteorological measurements are necessary to run single-point CLM simulations. Most inputs were available from alpine stations at Niwot Ridge (Figure 1), but we leveraged measurements from nearby subalpine stations as necessary. Specifically, we used air temperature, relative humidity, barometric pressure, and wind speed inputs measured at two alpine eddy covariance towers, which are located in fellfield and dry meadow vegetation (3480

164 m asl, AmeriFlux sites US-NR3 and US-NR4; Knowles, 2022a, 2022b; Knowles et al., 2012).
165 We used measurements from US-NR4 and gap-filled them using measurements from US-NR3
166 when necessary. Precipitation data came from the nearby Saddle site (3525 m asl) and were
167 corrected for the effects of blowing snow from October–May following Williams et al. (1998).
168 We used these data in combination with a half-hourly precipitation record from the subalpine
169 U.S. Climate Reference Network (USCRN) station 14W (40°02' N, 105°32' W; data from
170 <https://www.ncei.noaa.gov/pub/data/uscrn/products/subhourly01/>; accessed May 2022) measured
171 at 3050 m asl to distribute the Saddle precipitation record to the half-hour measurements needed
172 for CLM, following methods described in previous work (Wieder et al., 2017). Finally, incoming
173 shortwave radiation data were taken from a lower elevation eddy covariance tower, also located
174 in subalpine forest (Ameriflux site US-NR1, 3050 m asl; Burns et al., 2016), as incoming solar
175 measurements from higher elevations sites were not reliably collected over the alpine data record
176 (again, as in Wieder et al. 2017). Meteorological data were gap-filled using the R package
177 REddyProc (Wutzler et al., 2018).

178 We evaluated model results by comparing them with ongoing, publicly available Niwot
179 Ridge datasets, including snow depth collected ~biweekly from 88 gridded points since 1982
180 (Walker et al., 2022) and corresponding descriptions of dominant plant communities (Spasojevic
181 et al., 2013). We also compared our results with biomass harvests collected at the end of the
182 growing season to estimate annual aboveground net primary productivity (ANPP; Walker et al.,
183 2022). These ANPP measurements were multiplied by 0.5 to convert g dry weight to g C for
184 direct comparison with model outputs. For the dry meadow, we compared our simulations with
185 gross primary productivity (GPP) estimates from the alpine flux towers (Knowles, 2022a,
186 2022b). Finally, we used soil moisture and temperature data collected since 2018 from the

187 Sensor Network Array at Niwot Ridge (Morse & Niwot Ridge LTER, 2022) to evaluate our
188 simulations (Figure 1).



189 **Figure 1.** The Community Land Model (CLM) can be run at point scales and with site-specific
190 configurations to test ecological hypotheses using a combination of atmospheric forcings, plant
191 traits, and observational data for evaluation, as shown in this diagram of our model workflow for
192 single-point simulations with hillslope hydrology configured for an alpine tundra hillslope. (a)
193 shows the Niwot Ridge idealized hillslope, with separate columns for moist, wet, and dry
194 meadow vegetation. Black arrows indicate the direction of hydrologic connectivity with a
195 lowland (wet meadow) column connected to two upland (moist and dry meadow) columns.
196 Forcing data included meteorological measurements from two alpine flux towers (b, photo credit
197 J. Knowles), precipitation measurements from the Saddle site (c, photo credit W. Wieder; d,
198 photo credit J. Morse), and shortwave radiation measurements from the US-NR1 AmeriFlux
199 Tower site. Moist, wet, and dry meadows were parameterized using plant functional trait data
200 and phenocam observations (e) from Niwot Ridge. We used observational data from Niwot
201 Ridge including snow depth measurements, soil temperature and moisture from the Sensor
202 Network Array (f, aerial imagery from Wigmore & Niwot Ridge LTER, 2021), and aboveground
203 NPP measurements from biomass harvests to evaluate our results.

204
205

2.2 CLM overview

206 We ran single-point simulations of the CLM version 5 (Lawrence et al., 2019), the land
207 component of the Community Earth Systems Model (CESM; Danabasoglu et al., 2020), with the
208 hillslope hydrology configuration (Swenson et al., 2019) and active biogeochemistry, including

vertically resolved soil biogeochemistry (Koven et al., 2013) and site-level modifications to represent Niwot Ridge conditions. Our single-point CLM simulations approximate the footprint of an eddy covariance tower and allow ecological hypotheses to be tested and generated (Bonan et al., 2011; Hudiburg et al., 2013; Wieder et al., 2017). The hillslope hydrology configuration in CLM explicitly represents the effects of topography on insolation and the lateral redistribution of water at the scale of an average or ‘representative’ hillslope (Swenson et al., 2019).

For our representative hillslope at Niwot Ridge, we wanted to represent hydrological conditions at the well-studied Saddle site where topography and aspect control patterns of snow accumulation and vegetation distribution. To do this we implemented three hydrologically connected columns within the vegetated land unit, with one downslope ‘lowland’ column (wet meadow) and two upslope columns (moist and dry meadows; see Figure 1). In this configuration, surface and subsurface lateral flow was passed between neighboring columns and runoff from the lowland column was passed directly into the stream channel. See Swenson et al. (2019) for a detailed description of possible hillslope configurations and hillslope-scale hydrological processes in CLM. The number of columns within our hillslope and the connectivity between columns was prescribed by an input surface data set. The slope and aspect of each column was also prescribed by the surface data set, with the two upland columns having slopes of 0.3 m/m and east and west aspects (moist and dry meadow columns, respectively; Figure 1).

All simulations were spun up in “accelerated decomposition” mode for 200 years by cycling over four years of forcing data from 2008-2011; soil and vegetation C and N pools were then allowed to equilibrate for another 100 years (Lawrence et al., 2019). Historical simulations were conducted using observations of atmospheric data over the experimental period from 2008-2021. We ran historical simulations with fixed CO₂ concentrations.

2.2.1 Site-specific model setup

To better represent local conditions across vegetation communities in the Saddle, we made several site-specific modifications related to meteorological input data, surface characterizations, and parameterizations of the default Arctic C₃ grass plant functional type used in the CLM. Strong winds redistribute snow across Niwot Ridge (Erickson et al., 2005), leading to patchy distribution of snow that structures vegetation communities. Snow accumulates on leeward (east facing) slopes that support productive moist meadow communities with grasses (e.g., *Deschampsia caespitosa*) and forbs (e.g., *Acomastylis rossii*), whereas windward (west facing) slopes have little snow accumulation and support characteristic dry meadow communities dominated by sedges (e.g., *Kobresia myosuroides*). The physics of the CLM does not represent this fine scale, sub-grid redistribution of snow by wind, so we directly modified winter precipitation levels: when air temperatures were below 0°C, moist meadow columns, which accumulate the deepest winter snowpack, received 100% of observed Saddle precipitation, wet meadow columns received 75% of observed precipitation, and dry meadow columns received only 10% of observed precipitation. When air temperatures were above freezing all columns received identical precipitation (as rain). These modifications result in maximum snow depths that align with periodic snow depth measurements for these landscape positions that are collected across the Saddle grid and have been used in previous work at the site (Wieder et al., 2017).

Variations in soil properties across Niwot Ridge also reflect differences in snow accumulation and vegetation communities, with wetter parts of the landscape having deeper, more developed soils (Burns, 1980). Accordingly, we used National Ecological Observatory Network (NEON) Megapit data (Lombardozzi et al., 2023) to modify soil properties that reflect

these differences in soil characteristics seen in the field (Table S1). Specifically, for the rocky and less developed soils found in the dry meadow, we reduced water saturation by 50%. We also modified organic matter values based on data from Niwot Ridge (Burns, 1980) by reducing the organic matter fraction by 25% in moist and dry meadows to reflect that wet meadow soils have higher organic matter content than moist and dry meadows, and reduced sand content and increased clay content by 10% in the wet meadow. Lastly, we decreased the thickness of the dry surface layer, which controls soil evaporation (Swenson & Lawrence, 2014), by 33%.

Alpine tundra supports high floristic diversity with clear differences in functional traits that influence rates of photosynthesis and productivity in CLM (Fisher & Koven, 2020; Spasojevic et al., 2013). Accordingly, we modified foliar traits and phenology based on observations to represent moist, wet, and dry meadow vegetation (see Table S1). For foliar traits, we used functional trait data collected at Niwot Ridge over the past three decades (Spasojevic et al., 2013). We changed specific leaf area and foliar C:N ratios using median values calculated for each of the three communities. We also modified fine root to leaf allocation for each community based on observations and values from the literature (Table S1; Birch et al., 2021; Fisk et al., 1998). For phenology parameters, we used green chromatic coordinate (GCC) values extracted from phenocam observations from 2018-2022 at plots throughout the Saddle (Elwood et al., 2022) and phenometrics calculated from GCC values (unpublished data) to modify the timing of the growing season for each community. Phenometrics included start of growing season (50% of maximum GCC) and peak of growing season (maximum GCC) dates. We used 5 cm soil temperature observations and start of growing season dates in each community to calculate accumulated growing degree days (GDD; when surface soil temperatures $>0^{\circ}\text{C}$) before the start of leaf onset. Using these calculations, we modified a GDD scale factor in the model to represent

the increased GDD accumulation required in the dry meadow to trigger leaf out (a 70% increase compared to moist and wet meadows). We also calculated the number of days between leaf onset and peak greenness for each community (modifying *ndays_on* in Table S1).

When preliminary simulations showed high productivity biases compared to observations for all three communities, we modified several photosynthetic and plant hydraulic parameters to better represent alpine growth strategies (see Table S1). We first decreased two parameters in the mechanistic model of photosynthetic capacity used in CLM5 (leaf utilization of N for assimilation or LUNA; Ali et al., 2016) for all communities. These two parameters, j_{maxb0} and j_{maxb1} , specify the baseline proportion of N allocated for electron transport and the response of electron transport rate to light availability, respectively. To represent more conservative growth strategies in dry meadow vegetation, we decreased two plant hydraulic stress parameters representing maximum stem and root conductivity (Kennedy et al., 2019).

2.3 Model application and projection

After validating our model results against observations, we conducted two experimental simulations to quantify potential (1) effects of aspect on solar radiation that may moderate timing and magnitude of snowpack accumulation and runoff with cascading influences on soil moisture, soil temperature, and productivity on north and south facing slopes; and (2) interacting effects of aspect and climate change-induced warming across moist, wet, and dry meadows.

First, we ran two additional simulations to examine effects of aspect with the model setup as described above with several modifications. These simulations replicated the setup of our control (Saddle) simulations, except that the slope and aspect were modified to represent either a north or a south facing hillslope. We maintained the same precipitation inputs, vegetation

community parameterizations, and slope angle across all communities for consistency between control, south, and north facing simulations.

Second, to simulate climate change effects, we used an anomaly forcing protocol (Wieder et al. 2015), which provides a smooth transition between the observed alpine eddy covariance tower record (2008-2021) and a projected SSP3-7.0 scenario simulated by CESM2. Specifically, mean monthly changes (or anomalies) in the atmospheric state were calculated by subtracting the climatological mean of a ‘historic’ baseline, 2005-2014, from CESM2 projections under the SSP3-7.0 scenario through the end of the century. We added the atmospheric anomalies for the gridcell containing Niwot Ridge to meteorological data from the alpine flux tower that was cycled over the observational record. In addition to the atmospheric anomalies, the projected climate change scenario also included transient atmospheric CO₂ concentrations reaching 867 ppm by 2100 based on projected increases in emissions following protocols from the most recent Coupled Model Intercomparison Project (CMIP6) using CESM2. These future scenarios were run for all three vegetation communities on north and south facing aspects. We note that because climate trajectories may be accelerated at higher elevations (Mountain Research Initiative EDW Working Group, 2015; Wang et al., 2016), this approach represents a conservative estimate for changes in the mean atmospheric state that may be expected under this high emissions scenario. We also acknowledge that our approach represents a single possible climate change trajectory, but this balanced approach offers generalizable insight into how exposure to climate change may vary with aspect across topographically complex terrain.

3 Results and Discussion

3.1 Model evaluation: Niwot Ridge LTER measurements

Overall, the ecosystem-level CLM simulations agreed with observed patterns of soil

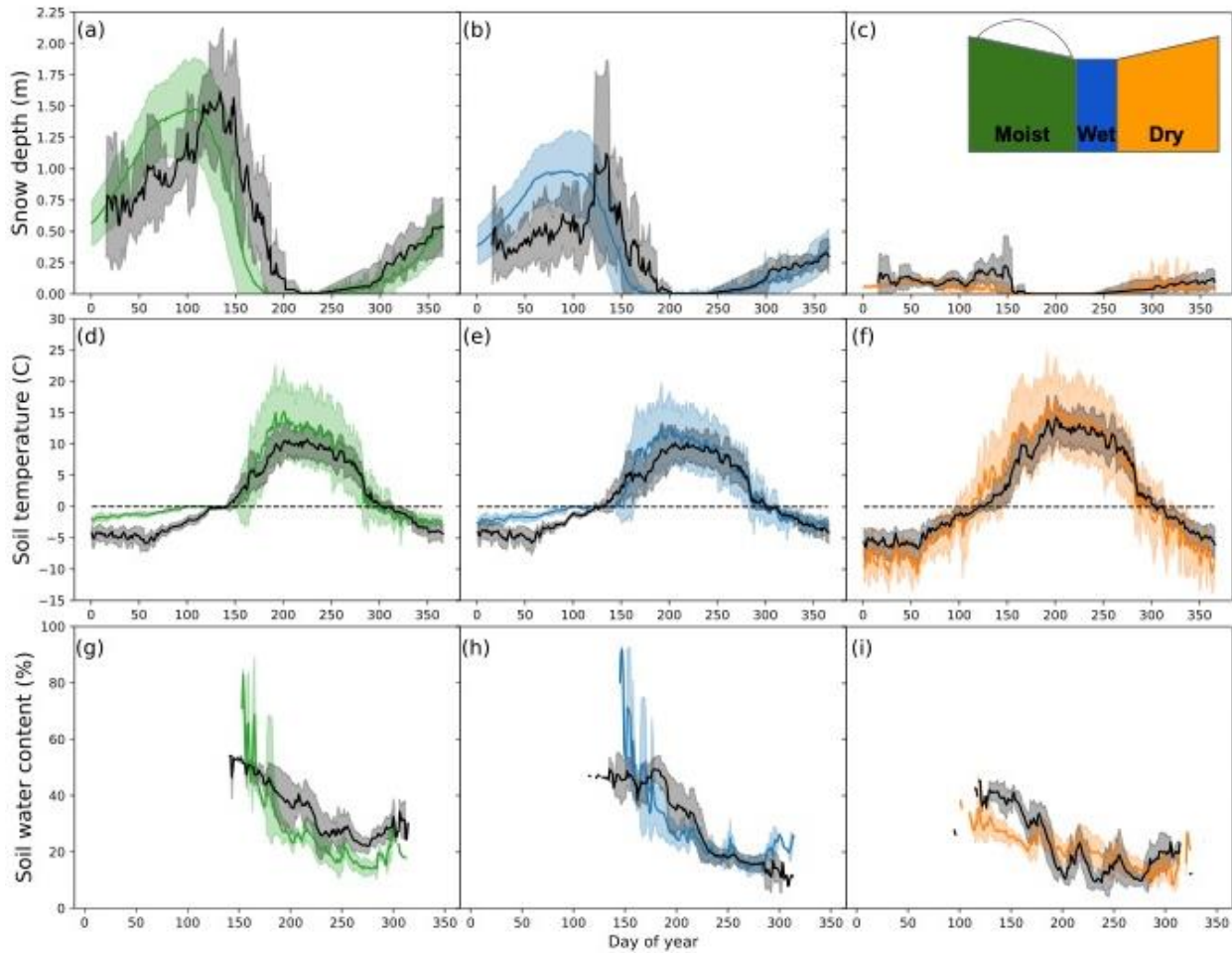
moisture, temperature, and snow depth from Niwot Ridge. Redistribution of snow by wind leads to three distinct vegetation communities that differ in their annual cycles of soil temperature, soil moisture, and productivity (Table 1), described in more detail below. Consistent with observations, simulated moist meadow and wet meadow communities are buffered from seasonal temperature extremes and remain relatively moist throughout their short growing season, whereas dry meadow communities experience wider seasonal fluctuations in soil temperature with longer, drier growing seasons.

Table 1. Comparison of key metrics related to snow, water, productivity, and soil conditions between moist, wet, and dry meadow communities from the Saddle (control) simulations with CLM. Growing season (GS) was defined where simulated GPP > 0. All values are means calculated from simulations over the alpine flux tower observational record (2008-2021). DOY stands for day of calendar year.

	Max. snow depth (m)	1st snow free DOY	GS length (days)	GPP (g C m⁻² y⁻¹)	Peak runoff DOY	GS soil moisture (%)	GS soil temp. (°C)
Moist	1.47	185	104.2	350.3	156	29.6	13.5
Wet	0.98	184	109.6	569.0	153	32.7	11.7
Dry	0.12	175	129.5	201.4	105	27.6	15.0

Modifications to winter precipitation allowed CLM simulations to capture observed gradients in snow accumulation across moist, wet, and dry meadows, as intended. Maximum snow depths simulated in each community (1.47 ± 0.55 m, 0.98 ± 0.36 m, and 0.12 ± 0.04 m in moist, wet, and dry meadow, respectively) corresponded well with observations across the Saddle grid (Table 1; Figure 2a-c). The simulations also captured interannual variability in snowpack across the 14-year measurement record (Figure S1). We found early biases in the timing of peak snow depth, initiation of snowmelt, and the first snow free day compared to

344 observations (Figure 2a-c). The first snow free day was ~20-30 days early in the moist and wet
 345 meadows, but values in the dry meadow matched observations more closely (Figure 2, Table 1).



346 **Figure 2.** Annual climatology of mean daily (\pm SD) (a-c) snow depth, (d-f) soil temperature (4
 347 cm depth), and (g-i) soil water content (4 cm depth; when soil temp. > 0) from CLM simulations
 348 configured for moist, wet, and dry meadow communities. Simulations and observations were
 349 averaged by day of year across 2008-2021 (snow depth) or 2017-2021 (soil temperature and
 350 water content) for each community, with dry, moist, and wet meadows in orange, green, and blue
 351 lines, respectively, and observations in black.

352
 353 Differences in timing between observations and simulations are unsurprising given the
 354 spatially and temporally variable nature of snow observations, which are particularly difficult to
 355 measure at high altitude sites with high wind transport (Williams et al., 1998). While CLM does
 356 not account for blowing snow, our simplified precipitation modifications resulted in a dry
 357 meadow snowpack that was thin and variable throughout the winter, as in the observations;

however, the simulations underestimated the effects of late spring storms, when heavier, higher-moisture snow can accumulate in windblown areas (Figure 2c). Early melt biases may also point to known shortcomings in the radiative transfer and albedo representation of snow in CLM. Indeed, proposed updates to the Snow, Ice, and Aerosol Radiative (SNICAR) module (Flanner et al., 2021) used in CLM offer promise—but additional work is needed to evaluate this scheme, which is outside the scope of this work. Our findings show that vegetation in CLM experiences snow-free conditions earlier in the growing season than actual plant communities at Niwot Ridge typically experience, but since soil temperature controls phenology for CLM Arctic C₃ grasses, the representation of soil temperature may be more important to consider than snow-free date.

Soil temperature and moisture simulated by the CLM broadly captured the climatological patterns observed among moist, wet, and dry meadows (Figure 2d-i), as well variation as between years (Figure S2). During winter months, moist and wet meadow soils remained near freezing due to the insulating effect of the snowpack, whereas snow-free dry meadow soils remained well below freezing. During the spring and summer, moist and wet meadow soils warmed later in the growing season (consistent with later snowmelt) and experienced lower maximum soil temperatures. By contrast, dry meadow soils warmed quickly in spring, resulting in a longer growing season with higher maximum summer temperatures (Table 1; Figure 2d-f). We found a bias towards warmer simulated soil temperatures (both winter and summer), notably in the moist and wet meadows (Figure 2d-e). Winter biases likely occurred due to the development of a deeper early season snowpack in moist and wet communities in CLM compared to observations (Figures 2a, 2b, and S1). Work at other sites suggests that snow thermal conductivity in CLM5 is too high, resulting in cold wintertime soil temperature biases (Dutch et al., 2022; Luo et al., 2023). Preliminary results from our simulations at Niwot Ridge,

however, suggest that thermal conductance of snow may be too low, resulting in warm winter soil temperature biases in moist and wet meadow columns.

Mean soil moisture (when soil temperatures were above 0°C) averaged $44.2 \pm 13.6\%$, $45 \pm 12.6\%$, and $31.7 \pm 6.2\%$ in moist, wet, and dry meadows, respectively, with moist and wet meadow soils maintaining higher soil moisture longer in the growing season than dry meadow soils (Figure 2g-i). As in previous modeling efforts at Niwot Ridge (Wieder et al., 2017), moist meadow soil moisture was primarily driven by snowmelt, whereas wet meadow soils received additional water subsidies from upslope areas, allowing them to maintain more moisture during the growing season (Figure 2g, 2h, and Table 1). By contrast, dry meadow soil moisture closely tracked episodic summer rainfall events (Figures 2i and S2f). In moist meadow sites, our simulations showed biases toward low soil moisture compared to observations. This could reflect a feedback between simulated soil hydrology and plant physiology, as higher than observed moist meadow productivity (Figure 3) may concurrently dry out soils in the model. Moreover, the soil hydraulic properties used in CLM may allow excess drainage in moist meadow soils and subsequent transfers to downslope wet meadow columns (although wet meadow soil moisture was also underestimated at this site). Meanwhile, in the dry meadow, CLM was unable to capture both the moisture peak following snowmelt and the magnitude of dry down throughout the growing season. Additional modifications to input data may better capture the late spring storms that led to deeper dry-meadow snow in the observations compared to our results (Figure 2c) and may improve dry meadow soil moisture early in the growing season. Moreover, our column-specific modifications to better represent rocky alpine soils (Table S1) in CLM may warrant further investigation for studies seeking higher fidelity simulations of soil abiotic conditions.

Broadly, our findings underscore the challenges of representing biophysical and biogeochemical processes in sophisticated land models with high dimensionality parameter space (Dagon et al., 2020). For example, the generalized pedotransfer functions that are used in global scale, coarse resolution climate simulations with CLM may need more careful evaluation for local application in ecosystem-scale studies (Dai et al., 2019; Luo et al., 2023). Such detailed measurements of soil thermal and hydraulic properties, however, are not commonly collected in sites with co-located measurements of plant traits (for model parameterization) and long-term measurements of ecosystem fluxes (for model calibration and evaluation). Indeed, even at a well-studied site such as Niwot Ridge, a paucity of data on soil physical properties precludes more robust interrogation of the belowground biases in our simulations. Moreover, the continuous, distributed measurements of soil temperature and moisture that we present are relatively new additions to the LTER data collections that began in 2018, following previous data-model integrations by Wieder et al. (2017). Given the harsh alpine environment, these data are hard-earned but likely inadequate to capture the high variability that characterizes soil moisture conditions across complex terrain (Loescher et al., 2014). Despite these challenges, our results demonstrate that the hillslope hydrology configuration of CLM can broadly represent meaningful abiotic conditions and ecological functions across a heterogeneous landscape.

Simulated estimates of both GPP and ANPP increased with moisture and snow depth across the tundra hillslope gradient (Figure 3 and Table 1), with mean annual GPP averaging 350 ± 45 , 569 ± 51 , and 201 ± 21 g C m⁻² yr⁻¹ in moist, wet, and dry meadow columns, respectively. Although moist meadow communities had the deepest snowpack, they were less productive than the wet meadow due to a shorter growing season (Figure 3 and Table 1). Wet meadow communities receive water subsidies from uphill columns, largely the moist meadow, and

experience little to no water stress during the growing season. On the other hand, dry meadow experiences the longest growing season and highest soil temperatures, but water limitation leads to more conservative growth strategies in this community (Spasojevic & Suding, 2012; Winkler et al., 2018). While simulated GPP values in the dry meadow were higher on average than the alpine flux tower observations (Figure 3b), they fell within the range of uncertainty, indicating that our simulations provide reasonable estimates of productivity (Figure 3a). Moreover, the footprint of the alpine flux towers includes significant areas of fellfield vegetation, which is heavily snow-scoured with very shallow, poorly developed soils, sparse vegetation cover, and lower productivity than dry meadow (Burns, 1980; Knowles et al., 2016; Wieder et al., 2017).

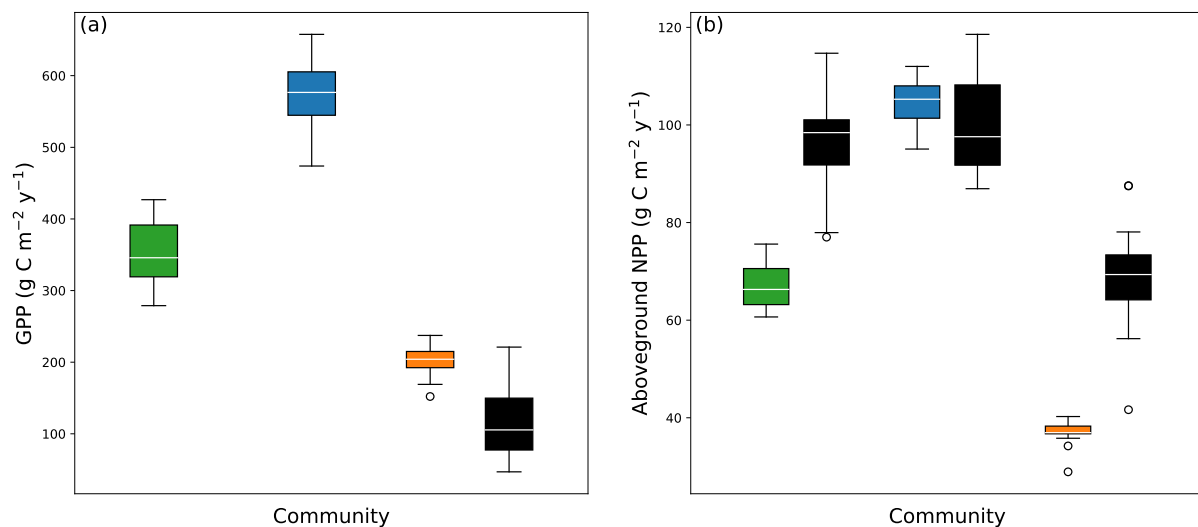


Figure 3. Boxplots of observed vs. simulated (a) mean annual gross primary productivity (GPP) and (b) aboveground net primary productivity (ANPP). Green, blue, and orange denote CLM simulations of moist, wet, and dry meadow communities, respectively, and black denotes observations from alpine flux towers (GPP, dry meadow only) and biomass harvests from the Saddle (ANPP), Niwot Ridge. Boxplot parameters throughout are as follows: median (white lines), interquartile range (boxes), and 1.5x interquartile range (whiskers).

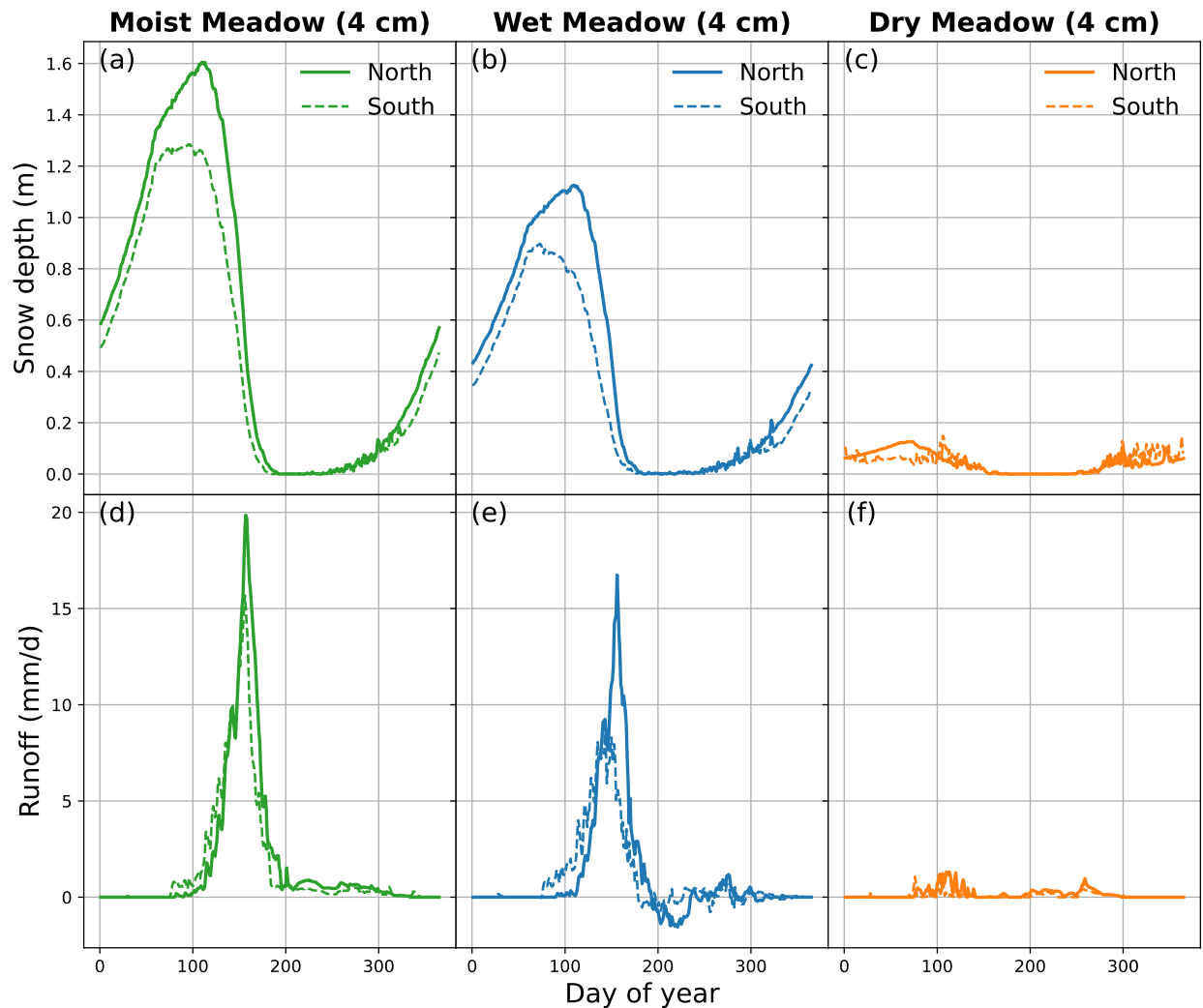
Without community-specific estimates of GPP, we calibrated model parameters to simulate differences in ANPP among vegetation communities, which our results broadly captured (Figure 3b). We found that the model underestimated ANPP by $\sim 30 \text{ g C m}^{-2} \text{ yr}^{-1}$ in moist and dry meadows compared to long-term measurements in the Saddle. A number of

parameters could be responsible for these biases. For example, compared to the default parameter in CLM5, we increased fine root C allocation relative to leaf C allocation, (Table S1), a modification supported by literature that demonstrates higher belowground C investment in arctic and alpine plants (Birch et al., 2021; Iversen et al., 2015; Jackson et al., 1996). Further modifications to the parameterizations of photosynthetic capacity, plant hydraulic stress, nutrient use efficiency, allocation, and turnover could further refine these results. Indeed, such efforts are the focus of ongoing work. Future work, therefore, should focus on quantifying broad plant functional traits for alpine vegetation and characterizing different growth strategies within and among tundra communities (Sulman et al., 2021). Broadly, however, our hillslope implementation of CLM5 adequately captured gradients in snow accumulation and ablation, soil temperature and moisture, and productivity that are observed among moist, wet, and dry meadow communities at Niwot Ridge. Next, we apply this modeling framework to investigate how aspect mediates ecosystem function in alpine tundra systems.

3.2 Model application: Aspect controls on hydrology, soil conditions, and growing season length

Leveraging novel capabilities of the hillslope hydrology configuration in CLM, we applied our modeling framework to investigate potential aspect-driven differences across topographically complex alpine landscapes. These north and south aspect simulations had the expected effect of decreasing snow depth on south aspects (Figure 4a-c and Table 2), indicating that higher winter solar radiation on south-facing slopes increases sublimation. During the spring, however, higher solar zenith angles reduce aspect-driven differences in solar radiation, which is the primary driver of ablation. Thus, our simulations showed negligible differences in

470 the timing of snowmelt between north- and south-facing simulations. Under current (2008-2021)
 471 conditions, only the moist meadow experienced delays in the first snow free day on north aspects
 472 compared to south aspects (Table 2). Deeper snowpack in the north aspect, however, did alter the
 473 timing and magnitude of runoff fluxes and transfers between hillslope columns. Peak runoff
 474 occurred later in north-facing columns, particularly in the wet meadow, which receives water
 475 subsidies from uphill moist meadow columns (Table 2; Figure 4d-f).



476 **Figure 4.** Mean annual climatology of snow depth (a-c) and runoff (d-f) from CLM simulations
 477 configured for north (solid lines) and south (dashed lines) aspects with moist (green lines), wet
 478 (blue lines), and dry (orange lines) meadow vegetation. Results were averaged by day of year
 479 across 2008-2021 study period for each community and aspect. Negative runoff values occur
 480 when inflow from uphill is greater than outflow.
 481

Despite similarities in snowmelt timing, we found that south aspects had longer growing seasons in all three communities (defined as the number of days when simulated GPP > 0). This occurred because south-facing soils warmed earlier than north-facing soils experiencing wetter, cooler conditions (Figure 5). Throughout the growing season, north-facing soils were 2.9, 3.5, and 2.2 °C cooler and 3.8, 3.8, and 4.2% wetter than south-facing soils in moist, wet, and dry meadows, respectively (Table 2), but the annual cycle of these differences varied (Figure 5). Specifically, the deep moist meadow snowpack buffered soils from aspect-driven differences in winter solar radiation, leading to negligible differences in winter soil temperatures between aspects (Figure 5a). Meanwhile, the dry meadow lacked this snow insulation and experienced warmer winter soil temperatures on south aspects (Figure 5c). Although south aspects had drier soils throughout the year, annual cycles of soil moisture were consistent between aspects in moist and dry meadows (Figure 5d, f). In contrast, the wet meadow had almost no aspect-driven difference in soil moisture early in the growing season, when runoff from the uphill moist meadow provided supplementary water inputs (Figure 4e); however, after day ~210 (late July), aspect effects emerged when south-facing soils dried out faster (Figure 5b). Overall, these differences in soil moisture and temperature highlight the role of aspect in controlling abiotic conditions across heterogeneous alpine environments (Isard, 1986), with implications for plant community composition and function. For example, in a subarctic forest-tundra ecotone, aspect was a stronger control on community composition than slope angle or elevation, driven by increased soil temperature and active layer depth (Dearborn & Danby, 2017). Similarly, our results suggest that historical snow accumulation patterns influence subsequent aspect-driven differences in soil temperature and moisture that may moderate how tundra vegetation experiences warming across heterogeneous alpine terrain.

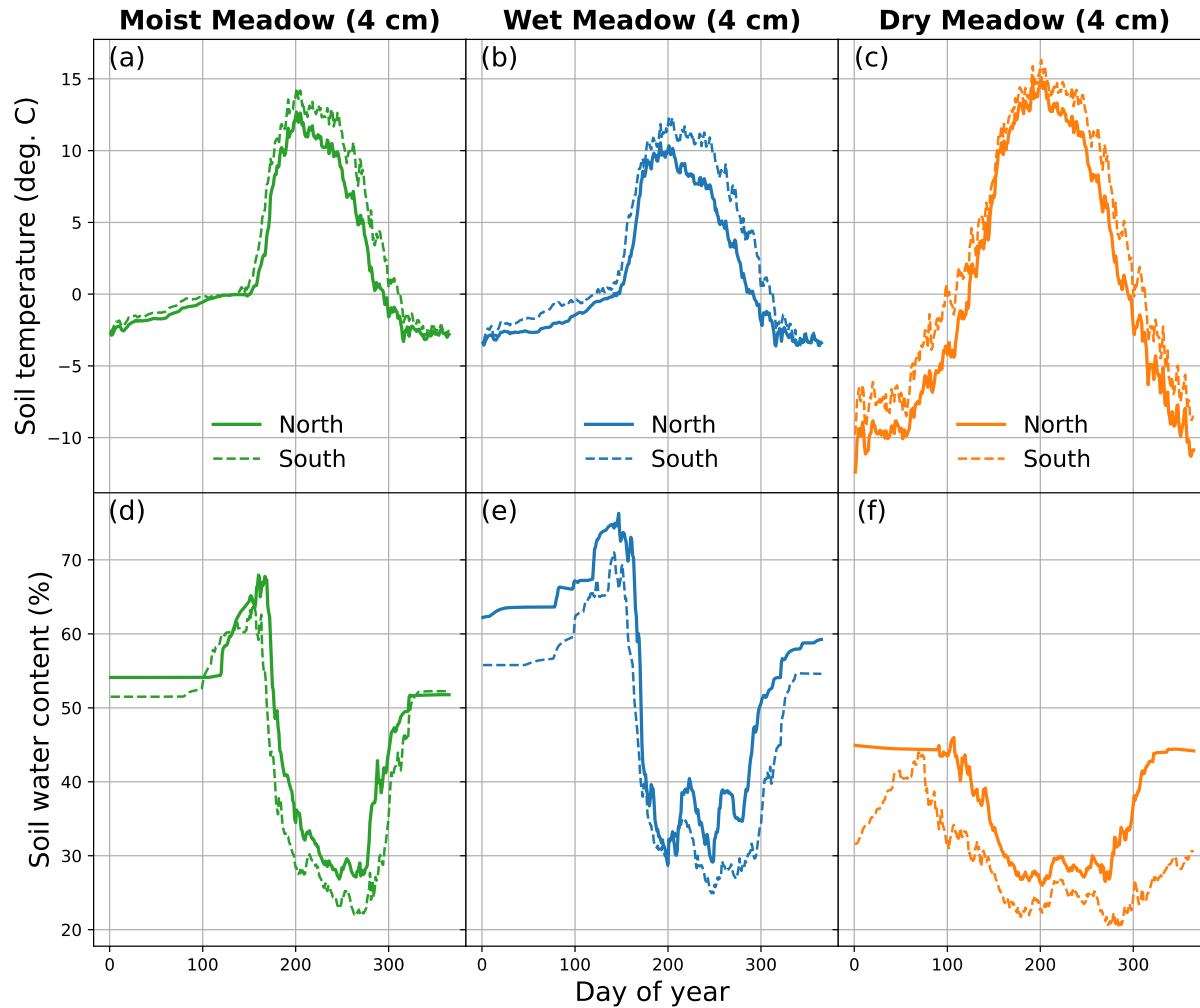


Figure 5. Mean annual climatology of soil temperature (a-c) and volumetric soil water content (d-f) at 4 cm depth from CLM simulations configured for north (solid lines) and south (dashed lines) aspects with moist (green lines), wet (blue lines), and dry (orange lines) meadow vegetation. Results were averaged by day of year across 2008-2021 study period for each community-aspect pairing.

Previous work on the impacts of topographic relief at hillslope scales indicates that warmer slopes should support longer growing seasons in areas with energy limitation, while cooler slopes can support higher productivity in areas with water limitation (Fan et al., 2019). Given that in our simulations, south aspects had longer growing seasons than north aspects (7-8% longer depending on community; Table 2), differences in cumulative GPP were surprising. Because moist meadow vegetation experiences a short growing season (May et al., 1982), we expected south aspects to have higher productivity, which was true, but only slightly (Figure

S3g, S3h; Table 2). These results align with the marginally earlier snowmelt date, higher soil temperature, and lower soil moisture conditions that characterized south-facing simulations (Figures 4-5). By contrast, north aspects were more productive in both wet (Figure 6g, 6h) and dry meadows (Figure S4g, S4h and Table 2). We suspect that growing season length is less limiting of wet and dry meadow, with soil N and water, respectively, providing larger constraints in CLM (as in Wieder et al. 2017). Moreover, the increase in wet and dry meadow productivity on north aspects may be a result of lower soil temperatures (Figure 5b) that reduce maintenance respiration (thereby increasing plant C use efficiency) or plant-soil feedbacks resulting from higher soil N stocks due to higher soil organic matter content simulated on north-facing slopes, which is also consistent with observations (Egli et al., 2009; Spasojevic et al., 2014).

3.3 Model projections: Alpine tundra responses to simulated warming and increased CO₂

To examine the role of microsite variation in potentially buffering alpine vegetation against climate change, we extended our simulations to year 2100 for all three communities on north- and south-facing aspects. The anomaly forcing from CESM2 included a 3.5°C warming of air temperature and an 8.2% increase in precipitation by 2100, relative to the historical baseline. These projected climate changes drove shifts in the timing of snow accumulation and ablation that had cascading effects on soil temperature, plant water availability, and productivity patterns, but the magnitude of these effects varied with landscape position. For brevity, we illustrate climate change effects on wet meadow columns (Figure 6), and present moist and dry meadow results in Table 2 and supplementary material (Figures S3-S4).

Table 2. Comparison of key metrics related to snow, water, productivity, and soil conditions between moist, wet, and dry meadow communities across north (N) and south (S) aspects for historical (2008-2021) and future (2086-2099) simulations. Growing season (GS) was defined where GPP > 0. DOY stands for day of calendar year.

Experiment			Max. snow depth (m)	1st snow free DOY	GS length (days)	GPP (g C m ⁻² y ⁻¹)	Peak runoff DOY	GS soil moisture (%)	GS soil temp. (°C)
Moist	S	Historical	1.28	184	107	363	155	28.7	14.8
		Future	1.27	165	125	631	135	26.8	17.6
	N	Historical	1.61	197	100	342	156	32.5	11.9
		Future	1.6	174	113	595	140	28.1	15.4
Wet	S	Historical	0.9	184	112	516	142	31.1	12.8
		Future	0.85	164	126	857	127	34.2	15.6
	N	Historical	1.13	184	105	628	155	35.0	9.4
		Future	1.1	164	115	997	142	33.3	13.0
Dry	S	Historical	0.15	167	137	241	105	24.2	15.4
		Future	0.16	152	150	403	69	21.3	18.4
	N	Historical	0.13	167	126	259	112	28.5	13.2
		Future	0.11	146	134	418	75	24.9	16.5

With projected warming, we found that the timing of snowmelt and runoff shifted earlier across all simulations, with concurrent decreases in maximum runoff rates. While maximum snow depth changed little between historical and future scenarios, the snowpack melted earlier in all future simulations (by 15-23 days depending on community and aspect; Table 2), leading to an 8-18% increase in growing season length, depending on location. Peak runoff was generally reduced and occurred earlier for all communities and aspects in future simulations (13-37 days earlier, with smaller and larger changes in wet meadow and dry meadows, respectively; Table 2), shifting the timing of runoff earlier relative to the start of the growing season (Figures 6c, 6d, S3c, S3d, S4c, and S4d). These changes in runoff timing and magnitude align with expectations and with previous modeling studies predicting that shallower snowpacks will melt earlier and more slowly across the Western U.S. (Clow, 2010; Musselman et al., 2017). However, an exception to the pattern of reduced runoff occurred in the south facing wet meadow, where peak runoff was approximately 20% higher in the future scenario (Figure 6c), peaking more quickly and being followed by a more rapid decline compared to the historical scenario. This increase

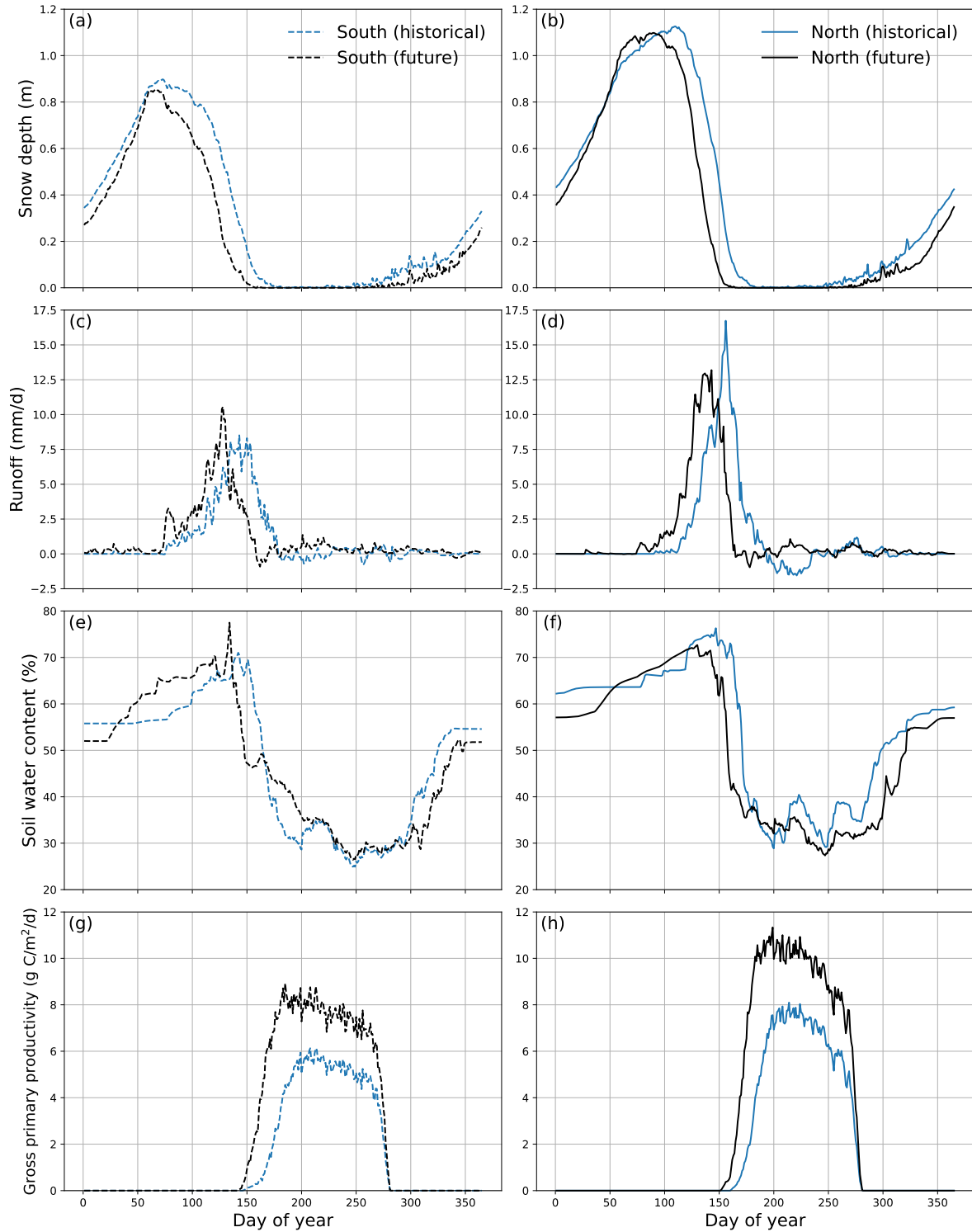


Figure 6. Mean annual climatology of (a, b) snow depth (m), (c, d) runoff (mm/d), (e, f) soil moisture (%), and (g, h) productivity in the wet meadow (lowland) column for historical (blue lines; 2008-2021) and future (black lines; 2086-2099) time periods. Results from south aspect (dashed lines) are shown in left column and those from north aspect (solid lines) are in right column. Values were averaged by day of year for each scenario and aspect. Negative runoff values occur when inflow from uphill is greater than outflow.

may be explained by a combination of factors including moist meadow water subsidies being passed downslope earlier (Figure S3), increased surface runoff due to lack of infiltration of snow-covered soils (Evans et al., 2018), and complex feedbacks between snow ablation rates, evapotranspiration, and plant water use (Barnhart et al., 2020; Harpold & Brooks, 2018).

Shifts in the timing and magnitude of snowmelt and runoff in our simulations suggest that plants are likely to experience decreased growing season water availability when demand is high, ultimately increasing plant water stress. These findings are consistent with previous modeling efforts at Niwot Ridge (Dong et al., 2019; Wieder et al., 2017) and measurements in a high-elevation Colorado wetland (Blanken, 2014). Seasonal snowmelt in alpine regions provides critical water resources in the Western U.S., but these high-elevations areas are particularly susceptible to climate change (Immerzeel et al., 2020; Mote et al., 2005). Water balance measurements in headwater catchments including Niwot Ridge have shown disproportionately high contributions of alpine tundra areas to total catchment discharge (Knowles et al., 2015), suggesting that these shifts in snowpack and runoff have significant implications for downstream water resources and hydrological processes.

Differences in the timing of snowmelt and runoff in our simulations led to shifts in growing season soil moisture and plant productivity across the hillslope gradient. In the moist and dry meadows, soils were consistently drier throughout the growing season in the future simulations (Figures S3e, S3f and S4e, S4f, Table 2). Indeed, dry meadow soil moisture patterns largely reflected episodic summer precipitation events, consistent with observations at the site (Figure 2i). The anomaly forcing approach we used cannot address potential changes in monsoon variability or strength that may be associated with climate change (Pascale et al., 2017), but our results underscore the importance of summer precipitation in determining plant water availability

in dry, and even moist meadow ecosystems. By contrast, because they received water subsidies from upslope, wet meadow soils were relatively buffered from changes in growing season soil moisture (Figure 6e and 6f). This finding is supported by previous work at Niwot Ridge emphasizing the role of snowmelt in shaping soil moisture in wetter areas (Taylor & Seastedt, 1994). We also found increased GPP in all communities in tandem with earlier snowmelt, drier soils, longer growing seasons, and increased atmospheric CO₂ concentrations (Figures 6, S3, and S4), although previous work has shown mixed productivity responses to warmer and drier conditions in tundra systems (Dong et al., 2019; Yang et al., 2020).

Simulated shifts in soil temperature and moisture varied with landscape position, with south aspects generally changing more than north aspects. We attributed these shifts to either aspect or community, depending on the metric, indicating that spatial heterogeneity can play a key role in moderating exposure to climate change. For example, south-facing dry meadow vegetation showed the biggest change in annual mean soil temperature and moisture in future simulations (Figure 7a, 7b). These changes in surface soil temperatures tracked the increase in air temperature from 2008-2100 (dashed line; Figure 7a). Previous work by Wentz et al., (2019) found that under current conditions dry meadow leaf temperatures were higher than in other communities and already near optimal values for photosynthesis, concluding that a 2°C air temperature increase would likely decrease carbon assimilation. In our simulations, dry meadow vegetation temperatures were approximately 1.7°C and 2.1°C higher than those in the moist and wet meadows, respectively. Our finding that soil temperatures track air temperatures in dry meadows suggests that these plants are likely more vulnerable to adverse effects of warming from climate change. In contrast, moist and wet meadow surface soil temperatures increased much less than air temperature due to the insulating effect of their deeper snowpack.

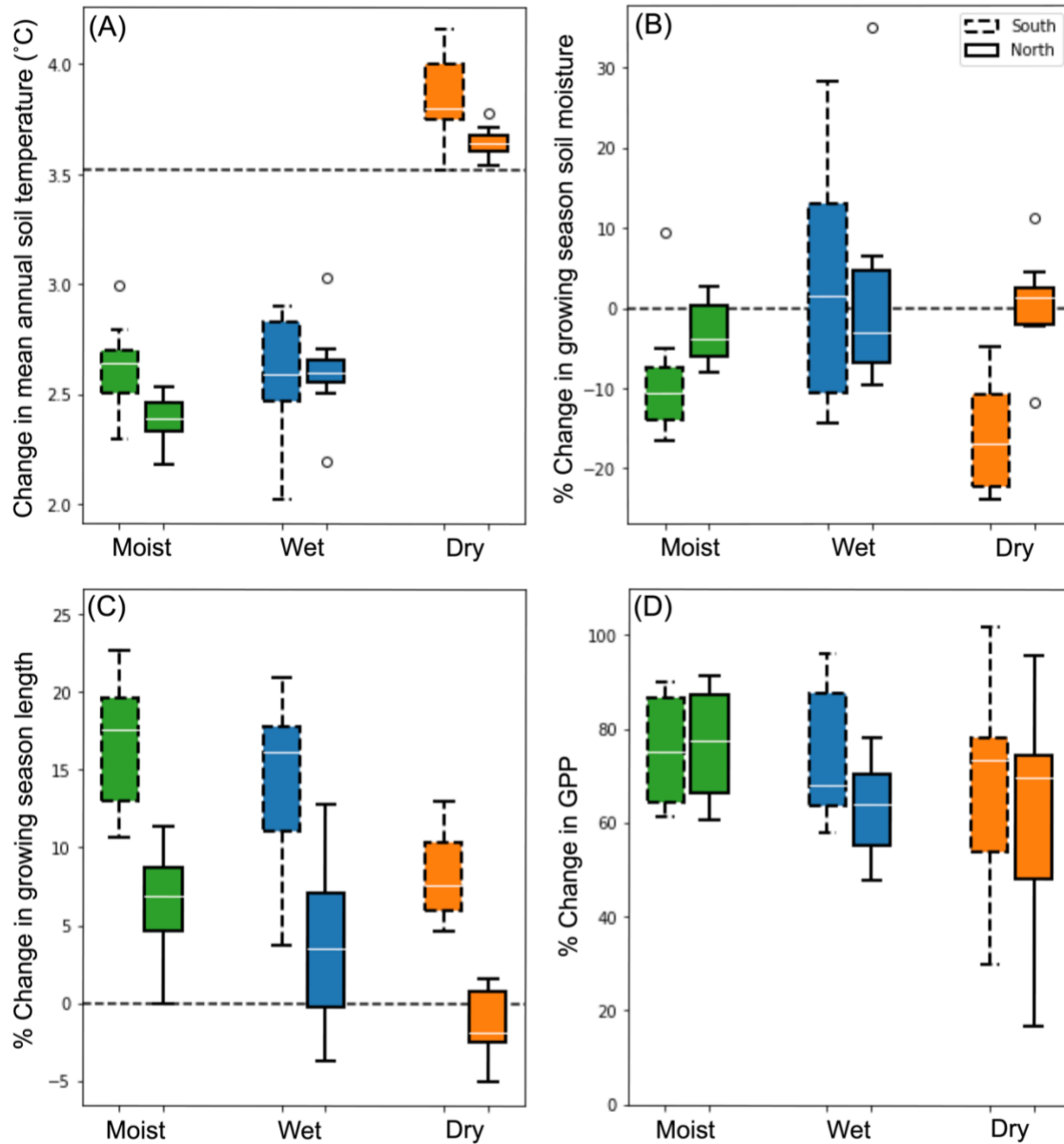


Figure 7. Metrics of climate change exposure and ecosystem services are moderated by community type and aspect in Niwot Ridge alpine tundra ecosystems. Boxplots show annual mean differences between corresponding years in the historical (2008-2015) and future (2092-2099) time periods for north (solid boxes) and south (dashed boxes) aspects. (a) change in mean annual surface soil temperature (dashed line represents the mean increase in air temperature between 2008 and 2100); (b) percent change in growing season soil moisture (normalized to soil moisture values for each community); (c) percent change in growing season length (normalized to growing season lengths for each community); and (d) percent change in gross primary productivity (normalized to productivity values from each community). Green, blue, and orange boxes represent, moist, wet, and dry communities, respectively.

Changes in growing season soil moisture and growing season length were primarily driven by aspect, with smaller differences among communities (Figure 7b-c). Soil moisture in south aspect dry meadow showed the greatest proportional decrease, followed by south aspect moist meadow. Aspect differences in soil moisture were not apparent in the wet meadow, where upslope water subsidies buffered against soil moisture change (Figure 7b). Likewise, increases in growing season length under climate change were more pronounced on south aspects (Figure 7c), with larger increases in moist and wet meadows due to earlier snowmelt (Table 2). Thus, our findings support the role of microclimates in moderating exposure and rates of response to climate change impacts that alpine vegetation may experience, where local conditions experienced by plants can be decoupled from atmospheric changes (Ackerly et al., 2020; Lenoir et al., 2013; Oldfather & Ackerly, 2019). Across the tundra hillslope gradient, differences in snowpack and hydrology dictated responses to warming, where cooler, wetter soils were maintained in lowland vegetation patches that accumulate moisture.

Our results suggest that abiotic shifts driven by changes in snowmelt timing are likely to alter resource connectivity across tundra ecosystems, where shifts in microbial biomass may lead to increased N export during snowmelt and decreased N available to alpine plants. In alpine areas where snow cover and cold soils result in short growing seasons (Billings & Mooney, 1968), lengthening the growing season may have outsized effects on microbial activity, nutrient cycling, and plant community dynamics. Microbial biomass typically peaks under spring snowpack (Lipson et al., 2000; Schadt et al., 2003), and shifts in soil microbial activity, biogeochemical cycling, and microbial community composition occur following snowmelt (Schmidt et al., 2015). For example, high microbial biomass under consistent snow cover buffers against inorganic N export during snowmelt (Brooks et al., 1998), and nutrients released as a result of microbial

activity following snowmelt are a key control on N availability to alpine plants (Lipson et al., 1999). Although our simulations are not well suited to explore these biotic feedbacks, our findings indicate that differences in aspect could moderate exposure to these changes.

In addition to longer growing seasons, we found increased productivity across all future simulations. These changes in GPP varied less between landscape positions than other metrics—all communities and aspects showed mean increases of similar magnitude (Figure 7d). However, GPP increases showed greater interannual variability in the dry meadow, supporting the idea that dry meadow experiences greater exposure to changes in abiotic conditions while moist and wet meadows are more buffered from these changes. In addition to warming effects, these GPP increases reflect greater atmospheric CO₂ concentrations that can lead to higher water use efficiency (Keenan et al., 2013) and higher photosynthetic rates per unit leaf area (Dong et al., 2019), which may help compensate for drier soils under the future climate scenario. In comparison to our findings (GPP increased from ~65-80%), Fan et al., (2016) parameterized an ecosystem biogeochemistry model for dry meadow tundra and found that a 3°C increase in soil and air temperature led to a corresponding ~50% GPP increase without accounting for increasing atmospheric CO₂. Although we lack observations to evaluate these results, our model evaluation efforts indicate relatively strong agreement between dry meadow simulations and flux tower GPP observations (Figure 3b). Furthermore, studies in arctic and alpine tundra have documented widespread shrubification (Formica et al., 2014; Sturm et al., 2001) and increases in graminoid abundance (Wookey et al., 2009), which tend to be accompanied by increased biomass and productivity and occur in tandem with global change factors. Elsewhere, studies also show that moisture limitation can exert strong controls on tundra productivity (Fan et al., 2016) and shrub growth and recruitment (Mekonnen et al., 2021), suggesting that declines in productivity and

shifts in plant community composition may occur in tundra sites experiencing greater soil moisture stress. Though our simulations are not suited to address effects of increased moisture stress on species composition, future efforts could leverage trait databases and ecosystem demography models to improve the representation of alpine plant functional types (Fisher & Koven, 2020) to explore more nuanced productivity responses to environmental change.

4 Conclusions

Overall, our findings highlight the value of incorporating site-level measurements into land models to ask ecological questions and improve projections of climate change impacts on ecosystem functions. Using local observations from Niwot Ridge and explicitly incorporating aspect effects on insolation and lateral hydrologic connectivity into our modeling framework, we found that leveraging the hillslope hydrology configuration within CLM allowed us to represent a topographically complex alpine environment. Our simulations captured gradients in snow accumulation, soil temperature and moisture, and productivity among hydrologically connected alpine vegetation communities and allowed us to examine aspect-driven differences and climate warming effects. Our findings demonstrate the role of local scale heterogeneity, including cooler north facing slopes and lowland areas that accumulate moisture, in buffering vegetation from experiencing warming and acting as potential refugia from climate change. Conversely, our findings highlight potential vulnerabilities of vegetation in dry, windblown, and south facing parts of the landscape that are less buffered from environmental change. To better understand how microscale variation will mediate rates of response to warming, future work should aim to better characterize growth strategies and plant functional traits within alpine vegetation and examine how shifts in these traits may mediate tundra responses to change. Interdisciplinary

approaches that combine site-level observations with modeling approaches are critical to investigate how rapid warming may alter ecosystem functions and services across topographically complex landscapes.

Acknowledgements

This research was supported by NSF grants DEB 1637686 and 2224439 to Niwot Ridge LTER. W. Wieder was also supported by NSF grants 1755088 and 2120804. We thank J. Morse, S. Aplet, and Niwot Ridge staff for project support as well as members of the Suding Lab for helpful discussions and feedback on earlier versions of this manuscript.

Open Research

Computing and data storage resources, including the Cheyenne supercomputer (<https://doi.org/10.5065/D6RX99HX>), were provided by the Computational and Information Systems Laboratory (CISL) at NCAR. Previous and current CLM versions are freely available at: <https://www.cesm.ucar.edu/models/clm>. The CLM5 data analyzed in this manuscript are in the process of being archived by the NCAR Digital Asset Services Hub (DASH; <https://data.ucar.edu>) and a doi will be provided when this process is complete. The data are temporarily available for download at: http://ftp.cgd.ucar.edu/pub/wwieder/NWT_CLM_cases.tar.gz. The code used to download data, run analyses, and produce graphics can be found on Zenodo at: <https://doi.org/10.5281/zenodo.8083491>.

References

- Ackerly, D. D., Kling, M. M., Clark, M. L., Papper, P., Oldfather, M. F., Flint, A. L., & Flint, L. E. (2020). Topoclimates, refugia, and biotic responses to climate change. *Frontiers in Ecology and the Environment*, 18(5), 288–297. <https://doi.org/10.1002/fee.2204>
- Alexander, J. M., Chalmandrier, L., Lenoir, J., Burgess, T. I., Essl, F., Haider, S., et al. (2018). Lags in the response of mountain plant communities to climate change. *Global Change Biology*, 24(2), 563–579. <https://doi.org/10.1111/gcb.13976>
- Ali, A. A., Xu, C., Rogers, A., Fisher, R. A., Wullschleger, S. D., Massoud, E. C., et al. (2016). A global scale mechanistic model of photosynthetic capacity (LUNA V1.0). *Geoscientific Model Development*, 9(2), 587–606. <https://doi.org/10.5194/gmd-9-587-2016>
- Barnhart, T. B., Tague, C. L., & Molotch, N. P. (2020). The Counteracting Effects of Snowmelt Rate and Timing on Runoff. *Water Resources Research*, 56(8), e2019WR026634. <https://doi.org/10.1029/2019WR026634>
- Billings, W. D., & Mooney, H. A. (1968). The ecology of arctic and alpine plants. *Biological Reviews*. Retrieved from <https://onlinelibrary.wiley.com/doi/abs/10.1111/j.1469-185X.1968.tb00968.x>
- Birch, L., Schwalm, C. R., Natali, S., Lombardozzi, D., Keppel-Aleks, G., Watts, J., et al. (2021). Addressing biases in Arctic–boreal carbon cycling in the Community Land Model Version 5. *Geoscientific Model Development*, 14(6), 3361–3382. <https://doi.org/10.5194/gmd-14-3361-2021>
- Blanken, P. D. (2014). The effect of winter drought on evaporation from a high-elevation wetland. *Journal of Geophysical Research: Biogeosciences*, 119(7), 1354–1369. <https://doi.org/10.1002/2014JG002648>

735 Bonan, G. B., Lawrence, P. J., Oleson, K. W., Levis, S., Jung, M., Reichstein, M., et al. (2011).
 736 Improving canopy processes in the Community Land Model version 4 (CLM4) using
 737 global flux fields empirically inferred from FLUXNET data. *Journal of Geophysical*
 738 *Research: Biogeosciences*, 116(G2), 1–22. <https://doi.org/10.1029/2010JG001593>
 739 Brooks, P. D., Williams, M. W., & Schmidt, S. K. (1998). Inorganic nitrogen and microbial
 740 biomass dynamics before and during spring snowmelt. *Biogeochemistry*, 43(1), 1–15.
 741 <https://doi.org/10.1023/A:1005947511910>
 742 Bueno de Mesquita, C. P., White, C. T., Farrer, E. C., Hallett, L. M., & Suding, K. N. (2021).
 743 Taking climate change into account: Non-stationarity in climate drivers of ecological
 744 response. *Journal of Ecology*, 109(3), 1491–1500. [https://doi.org/10.1111/1365-](https://doi.org/10.1111/1365-2745.13572)
 745 [2745.13572](https://doi.org/10.1111/1365-2745.13572)
 746 Burns, S. F. (1980). *Alpine soil distribution and development, Indian Peaks, Colorado Front*
 747 *Range*,. University of Colorado, Boulder, CO.
 748 Burns, S. P., Maclean, G. D., Blanken, P. D., Oncley, S. P., Semmer, S. R., & Monson, R. K.
 749 (2016). The Niwot Ridge Subalpine Forest US-NR1 AmeriFlux site – Part 1: Data
 750 acquisition and site record-keeping. *Geoscientific Instrumentation, Methods and Data*
 751 *Systems*, 5(2), 451–471. <https://doi.org/10.5194/gi-5-451-2016>
 752 Caine, N. (1996). Streamflow patterns in the alpine environment of North Boulder Creek,
 753 Colorado Front Range. *Streamflow Patterns in the Alpine Environment of North Boulder*
 754 *Creek, Colorado Front Range*, (104), 27–42.
 755 Chen, Y., Wieder, W. R., Hermes, A. L., & Hinckley, E.-L. S. (2020). The role of physical
 756 properties in controlling soil nitrogen cycling across a tundra-forest ecotone of the

757 Colorado Rocky Mountains, U.S.A. *CATENA*, 186, 104369.
 758 <https://doi.org/10.1016/j.catena.2019.104369>

759 Christianson, K. R., Loria, K. A., Blanken, P. D., Caine, N., & Johnson, P. T. J. (2021). On thin
 760 ice: Linking elevation and long-term losses of lake ice cover. *Limnology and*
 761 *Oceanography Letters*, 6(2), 77–84. <https://doi.org/10.1002/lol2.10181>

762 Clow, D. W. (2010). Changes in the timing of snowmelt and streamflow in Colorado: A response
 763 to recent warming. *Journal of Climate*, 23(9), 2293–2306.
 764 <https://doi.org/10.1175/2009JCLI2951.1>

765 Dagon, K., Sanderson, B. M., Fisher, R. A., & Lawrence, D. M. (2020). A machine learning
 766 approach to emulation and biophysical parameter estimation with the Community Land
 767 Model, version 5. *Advances in Statistical Climatology, Meteorology and Oceanography*,
 768 6, 223–244. <https://doi.org/10.5194/ascmo-6-223-2020>

769 Dai, Y., Xin, Q., Wei, N., Zhang, Y., Shangguan, W., Yuan, H., et al. (2019). A global high-
 770 resolution data set of soil hydraulic and thermal properties for land surface modeling.
 771 *Journal of Advances in Modeling Earth Systems*, 11(9), 2996–3023.
 772 <https://doi.org/10.1029/2019MS001784>

773 Danabasoglu, G., Lamarque, J. -F., Bacmeister, J., Bailey, D. A., DuVivier, A. K., Edwards, J.,
 774 et al. (2020). The Community Earth System Model Version 2 (CESM2). *Journal of*
 775 *Advances in Modeling Earth Systems*, 12(2). <https://doi.org/10.1029/2019MS001916>

776 Daubenmire, R. F. (1943). Vegetational Zonation in the Rocky Mountains. *Botanical Review*,
 777 9(6), 325–393.

778 Dearborn, K. D., & Danby, R. K. (2017). Aspect and slope influence plant community
779 composition more than elevation across forest–tundra ecotones in subarctic Canada.
780 *Journal of Vegetation Science*, 28(3), 595–604.

781 Dong, Z., Driscoll, C. T., Campbell, J. L., Pourmokhtarian, A., Stoner, A. M. K., & Hayhoe, K.
782 (2019). Projections of water, carbon, and nitrogen dynamics under future climate change
783 in an alpine tundra ecosystem in the southern Rocky Mountains using a biogeochemical
784 model. *Science of The Total Environment*, 650, 1451–1464.
785 <https://doi.org/10.1016/j.scitotenv.2018.09.151>

786 Dutch, V. R., Rutter, N., Wake, L., Sandells, M., Derksen, C., Walker, B., et al. (2022). Impact
787 of measured and simulated tundra snowpack properties on heat transfer. *The Cryosphere*,
788 16(10), 4201–4222. <https://doi.org/10.5194/tc-16-4201-2022>

789 Egli, M., Sartori, G., Mirabella, A., Favilli, F., Giacciai, D., & Delbos, E. (2009). Effect of north
790 and south exposure on organic matter in high alpine soils. *Geoderma*, 149(1), 124–136.
791 <https://doi.org/10.1016/j.geoderma.2008.11.027>

792 Elwood, K. K., Smith, J. G., Elmendorf, S. C., & Niwot Ridge LTER. (2022). *Time-lapse*
793 *camera (phenocam) imagery of sensor network plots, 2017 - ongoing. ver 3.*
794 Environmental Data Initiative. Retrieved from
795 <https://doi.org/10.6073/pasta/285918fbf5cc4bd2ed2c1241db9a1b2d>

796 Erickson, T. A., Williams, M. W., & Winstral, A. (2005). Persistence of topographic controls on
797 the spatial distribution of snow in rugged mountain terrain, Colorado, United States.
798 *Water Resources Research*, 41(4). <https://doi.org/10.1029/2003WR002973>

799 Ernakovich, J. G., Hopping, K. A., Berdanier, A. B., Simpson, R. T., Kachergis, E. J., Steltzer,
800 H., & Wallenstein, M. D. (2014). Predicted responses of arctic and alpine ecosystems to

801 altered seasonality under climate change. *Global Change Biology*, 20(10), 3256–3269.
 802 <https://doi.org/10.1111/gcb.12568>
 803 Evans, S. G., Ge, S., Voss, C. I., & Molotch, N. P. (2018). The role of frozen soil in groundwater
 804 discharge predictions for warming alpine watersheds. *Water Resources Research*, 54(3),
 805 1599–1615. <https://doi.org/10.1002/2017WR022098>
 806 Fan, Y., Clark, M., Lawrence, D. M., Swenson, S., Band, L. E., Brantley, S. L., et al. (2019).
 807 Hillslope hydrology in global change research and Earth System Modeling. *Water*
 808 *Resources Research*, 55(2), 1737–1772. <https://doi.org/10.1029/2018WR023903>
 809 Fan, Z., Neff, J. C., & Wieder, W. R. (2016). Model-based analysis of environmental controls
 810 over ecosystem primary production in an alpine tundra dry meadow. *Biogeochemistry*,
 811 128(1), 35–49. <https://doi.org/10.1007/s10533-016-0193-9>
 812 Fisher, R. A., & Koven, C. D. (2020). Perspectives on the future of land surface models and the
 813 challenges of representing complex terrestrial systems. *Journal of Advances in Modeling*
 814 *Earth Systems*, 12(4), e2018MS001453. <https://doi.org/10.1029/2018MS001453>
 815 Fisk, M. C., Schmidt, S. K., & Seastedt, T. R. (1998). Topographic patterns of above- and
 816 belowground Production and nitrogen cycling in alpine tundra. *Ecology*, 79(7), 2253–
 817 2266. [https://doi.org/10.1890/0012-9658\(1998\)079\[2253:TPOAAB\]2.0.CO;2](https://doi.org/10.1890/0012-9658(1998)079[2253:TPOAAB]2.0.CO;2)
 818 Flanner, M. G., Arnheim, J. B., Cook, J. M., Dang, C., He, C., Huang, X., et al. (2021).
 819 SNICAR-ADv3: a community tool for modeling spectral snow albedo. *Geoscientific*
 820 *Model Development*, 14(12), 7673–7704. <https://doi.org/10.5194/gmd-14-7673-2021>
 821 Formica, A., Farrer, E. C., Ashton, I. W., & Suding, K. N. (2014). Shrub expansion over the past
 822 62 years in Rocky Mountain alpine tundra: Possible causes and consequences. *Arctic*,

823 *Antarctic, and Alpine Research*, 46(3), 616–631. <https://doi.org/10.1657/1938-4246->
824 46.3.616

825 Harpold, A. A., & Brooks, P. D. (2018). Humidity determines snowpack ablation under a
826 warming climate. *Proceedings of the National Academy of Sciences*, 115(6), 1215–1220.
827 <https://doi.org/10.1073/pnas.1716789115>

828 Helm, D. (1982). Multivariate Analysis of Alpine Snow-Patch Vegetation Cover near Milner
829 Pass, Rocky Mountain National Park, Colorado, U.S.A. *Arctic and Alpine Research*,
830 14(2), 87–95. <https://doi.org/10.1080/00040851.1982.12004285>

831 Hermes, A. L., Wainwright, H. M., Wigmore, O., Falco, N., Molotch, N. P., & Hinckley, E.-L. S.
832 (2020). From Patch to Catchment: A Statistical Framework to Identify and Map Soil
833 Moisture Patterns Across Complex Alpine Terrain. *Frontiers in Water*, 2, 578602.
834 <https://doi.org/10.3389/frwa.2020.578602>

835 Hinckley, E. S., Ebel, B. A., Barnes, R. T., Anderson, R. S., Williams, M. W., & Anderson, S. P.
836 (2012). Aspect control of water movement on hillslopes near the rain– snow transition of
837 the Colorado Front Range. *Hydrological Processes*, 28(1), 74–85.
838 <https://doi.org/10.1002/hyp.9549>

839 Hock, R., Rasul, G., Adler, C., Cáceres, B., Gruber, S., Hirabayashi, Y., et al. (2019). *IPCC*
840 *special report: High Mountain Areas, IPCC Special Report on the Ocean and*
841 *Cryosphere in a Changing Climate*.

842 Hudiburg, T. W., Law, B. E., & Thornton, P. E. (2013). Evaluation and improvement of the
843 Community Land Model (CLM4) in Oregon forests. *Biogeosciences*, 10(1), 453–470.
844 <https://doi.org/10.5194/bg-10-453-2013>

845 Immerzeel, W. W., Lutz, A. F., Andrade, M., Bahl, A., Biemans, H., Bolch, T., et al. (2020).
 846 Importance and vulnerability of the world's water towers. *Nature*, 577(7790), 364–369.
 847 <https://doi.org/10.1038/s41586-019-1822-y>
 848 Isard, S. A. (1986). Factors influencing soil moisture and plant community distribution on Niwot
 849 Ridge, Front Range, Colorado, U.S.A. *Arctic and Alpine Research*, 18(1), 83–96.
 850 <https://doi.org/10.1080/00040851.1986.12004065>
 851 Iversen, C. M., Sloan, V. L., Sullivan, P. F., Euskirchen, E. S., McGuire, A. D., Norby, R. J., et
 852 al. (2015). The unseen iceberg: plant roots in arctic tundra. *New Phytologist*, 205(1), 34–
 853 58. <https://doi.org/10.1111/nph.13003>
 854 Jackson, R. B., Canadell, J., Ehleringer, J. R., Mooney, H. A., Sala, O. E., & Schulze, E. D.
 855 (1996). A global analysis of root distributions for terrestrial biomes. *Oecologia*, 108(3),
 856 389–411. <https://doi.org/10.1007/BF00333714>
 857 Keenan, T. F., Hollinger, D. Y., Bohrer, G., Dragoni, D., Munger, J. W., Schmid, H. P., &
 858 Richardson, A. D. (2013). Increase in forest water-use efficiency as atmospheric carbon
 859 dioxide concentrations rise. *Nature*, 499(7458), 324–327.
 860 <https://doi.org/10.1038/nature12291>
 861 Kennedy, D., Swenson, S., Oleson, K. W., Lawrence, D. M., Fisher, R., Lola da Costa, A. C., &
 862 Gentine, P. (2019). Implementing plant hydraulics in the Community Land Model,
 863 version 5. *Journal of Advances in Modeling Earth Systems*, 11(2), 485–513.
 864 <https://doi.org/10.1029/2018MS001500>
 865 Kittel, T. G. F., Williams, M. W., Chowanski, K., Hartman, M., Ackerman, T., Losleben, M., &
 866 Blanken, P. D. (2015). Contrasting long-term alpine and subalpine precipitation trends in

a mid-latitude North American mountain system, Colorado Front Range, USA. *Plant Ecology & Diversity*, 8(5–6), 607–624. <https://doi.org/10.1080/17550874.2016.1143536>

Knowles, J. F. (2022a). *AmeriFlux BASE US-NR3 Niwot Ridge Alpine (T-Van West), Ver. 3-5, AmeriFlux AMP, (Dataset)*. Retrieved from <https://doi.org/10.17190/AMF/1804491>

Knowles, J. F. (2022b). *AmeriFlux BASE US-NR4 Niwot Ridge Alpine (T-Van East), Ver. 3-5, AmeriFlux AMP, (Dataset)*. Retrieved from <https://doi.org/10.17190/AMF/1804492>

Knowles, J. F., Blanken, P. D., Williams, M. W., & Chowanski, K. M. (2012). Energy and surface moisture seasonally limit evaporation and sublimation from snow-free alpine tundra. *Agricultural and Forest Meteorology*, 157, 106–115. <https://doi.org/10.1016/j.agrformet.2012.01.017>

Knowles, J. F., Harpold, A. A., Cowie, R., Zeliff, M., Barnard, H. R., Burns, S. P., et al. (2015). The relative contributions of alpine and subalpine ecosystems to the water balance of a mountainous, headwater catchment. *Hydrological Processes*, 29(22), 4794–4808. <https://doi.org/10.1002/hyp.10526>

Knowles, J. F., Blanken, P. D., & Williams, M. W. (2016). Wet meadow ecosystems contribute the majority of overwinter soil respiration from snow-scoured alpine tundra. *Journal of Geophysical Research: Biogeosciences*, 121(4), 1118–1130. <https://doi.org/10.1002/2015JG003081>

Knowles, J. F., Blanken, P. D., Lawrence, C. R., & Williams, M. W. (2019). Evidence for non-steady-state carbon emissions from snow-scoured alpine tundra. *Nature Communications*, 10(1), 1306. <https://doi.org/10.1038/s41467-019-09149-2>

Körner, C., & Hiltbrunner, E. (2021). Why Is the Alpine Flora Comparatively Robust against Climatic Warming? *Diversity*, 13(8), 383. <https://doi.org/10.3390/d13080383>

- Koven, C. D., Riley, W. J., Subin, Z. M., Tang, J. Y., Torn, M. S., Collins, W. D., et al. (2013). The effect of vertically resolved soil biogeochemistry and alternate soil C and N models on C dynamics of CLM4. *Biogeosciences*, 10(11), 7109–7131. <https://doi.org/10.5194/bg-10-7109-2013>
- Lawrence, D. M., Fisher, R. A., Koven, C. D., Oleson, K. W., Swenson, S. C., Bonan, G., et al. (2019). The Community Land Model Version 5: Description of new features, benchmarking, and impact of forcing uncertainty. *Journal of Advances in Modeling Earth Systems*, 11(12), 4245–4287. <https://doi.org/10.1029/2018MS001583>
- Lenoir, J., Graae, B. J., Aarrestad, P. A., Alsos, I. G., Armbruster, W. S., Austrheim, G., et al. (2013). Local temperatures inferred from plant communities suggest strong spatial buffering of climate warming across Northern Europe. *Global Change Biology*, 19(5), 1470–1481. <https://doi.org/10.1111/gcb.12129>
- Lenoir, J., Hattab, T., & Pierre, G. (2017). Climatic microrefugia under anthropogenic climate change: implications for species redistribution. *Ecography*, 40(2), 253–266. <https://doi.org/10.1111/ecog.02788>
- Lipson, D. A., Schmidt, S. K., & Monson, R. K. (1999). Links between microbial population dynamics and Nitrogen availability in an alpine ecosystem. *Ecology*, 80(5), 1623–1631. [https://doi.org/10.1890/0012-9658\(1999\)080\[1623:LBMPDA\]2.0.CO;2](https://doi.org/10.1890/0012-9658(1999)080[1623:LBMPDA]2.0.CO;2)
- Lipson, D. A., Schmidt, S. K., & Monson, R. K. (2000). Carbon availability and temperature control the post-snowmelt decline in alpine soil microbial biomass. *Soil Biology and Biochemistry*, 32(4), 441–448. [https://doi.org/10.1016/S0038-0717\(99\)00068-1](https://doi.org/10.1016/S0038-0717(99)00068-1)
- Litaor, M. I., Williams, M., & Seastedt, T. R. (2008). Topographic controls on snow distribution, soil moisture, and species diversity of herbaceous alpine vegetation, Niwot Ridge,

Colorado. *Journal of Geophysical Research: Biogeosciences*, 113(G2).
<https://doi.org/10.1029/2007JG000419>

Loescher, H., Ayres, E., Duffy, P., Luo, H., & Brunke, M. (2014). Spatial variation in soil properties among North American ecosystems and guidelines for sampling designs. *PLOS ONE*, 9(1), e83216. <https://doi.org/10.1371/journal.pone.0083216>

Lombardozzi, D. L., Wieder, W. R., Sobhani, N., Bonan, G. B., Durden, D., Lenz, D., et al. (2023). *Overcoming barriers to enable convergence research by integrating ecological and climate sciences: The NCAR-NEON system Version 1* (preprint). Earth and space science informatics. <https://doi.org/10.5194/egusphere-2023-271>

Luo, J., Huang, A., Lyu, S., Lin, Z., Gu, C., Li, Z., et al. (2023). Improved Performance of CLM5.0 Model in Frozen Soil Simulation Over Tibetan Plateau by Implementing the Vegetation Emissivity and Gravel Hydrothermal Schemes. *Journal of Geophysical Research: Atmospheres*, 128(6), e2022JD038021. <https://doi.org/10.1029/2022JD038021>

Mao, J., Ricciuto, D. M., Thornton, P. E., Warren, J. M., King, A. W., Shi, X., et al. (2016). Evaluating the Community Land Model in a pine stand with shading manipulations and ¹³CO₂ labeling. *Biogeosciences*, 13(3), 641–657. <https://doi.org/10.5194/bg-13-641-2016>

May, D. E., Webber, P. J., & May, T. A. (1982). Success of Transplanted Alpine Tundra Plants on Niwot Ridge, Colorado. *Journal of Applied Ecology*, 19(3), 965–976.

McGuire, C. R., Nufio, C. R., Bowers, M. D., & Guralnick, R. P. (2012). Elevation-dependent temperature trends in the Rocky Mountain Front Range: Changes over a 56- and 20-year record. *PLOS ONE*, 7(9), e44370. <https://doi.org/10.1371/journal.pone.0044370>

934 McLaughlin, B. C., Ackerly, D. D., Klos, P. Z., Natali, J., Dawson, T. E., & Thompson, S. E.
 935 (2017). Hydrologic refugia, plants, and climate change. *Global Change Biology*, 23(8),
 936 2941–2961. <https://doi.org/10.1111/gcb.13629>
 937 Mekonnen, Z. A., Riley, W. J., Berner, L. T., Bouskill, N. J., Torn, M. S., Iwahana, G., et al.
 938 (2021). Arctic tundra shrubification: a review of mechanisms and impacts on ecosystem
 939 carbon balance. *Environmental Research Letters*, 16(5), 053001.
 940 <https://doi.org/10.1088/1748-9326/abf28b>
 941 Morse, J. F., & Niwot Ridge LTER. (2022). *Climate data for saddle catchment sensor network,*
 942 *2017 - ongoing. ver 4.* Environmental Data Initiative. Retrieved from
 943 <https://doi.org/10.6073/pasta/598894834ea3bae61d7550c30da06565>
 944 Mote, P. W., Hamlet, A. F., Clark, M. P., & Lettenmaier, D. P. (2005). Declining mountain
 945 snowpack in western North America. *Bulletin of the American Meteorological Society*,
 946 86(1), 39–50. <https://doi.org/10.1175/BAMS-86-1-39>
 947 Mountain Research Initiative EDW Working Group. (2015). Elevation-dependent warming in
 948 mountain regions of the world. *Nature Climate Change*, 5(5), 424–430.
 949 <https://doi.org/10.1038/nclimate2563>
 950 Musselman, K. N., Clark, M. P., Liu, C., Ikeda, K., & Rasmussen, R. (2017). Slower snowmelt
 951 in a warmer world. *Nature Climate Change*, 7(3), 214–219.
 952 <https://doi.org/10.1038/nclimate3225>
 953 Musselman, K. N., Addor, N., Vano, J. A., & Molotch, N. P. (2021). Winter melt trends portend
 954 widespread declines in snow water resources. *Nature Climate Change*, 11, 418–424.
 955 <https://doi.org/10.1038/s41558-021-01014-9>

956 Oldfather, M. F., & Ackerly, D. D. (2019). Microclimate and demography interact to shape
 957 stable population dynamics across the range of an alpine plant. *New Phytologist*, 222(1),
 958 193–205. <https://doi.org/10.1111/nph.15565>
 959 Opedal, Ø. H., Armbruster, W. S., & Graae, B. J. (2015). Linking small-scale topography with
 960 microclimate, plant species diversity and intra-specific trait variation in an alpine
 961 landscape. *Plant Ecology & Diversity*, 8(3), 305–315.
 962 <https://doi.org/10.1080/17550874.2014.987330>
 963 Panetta, A. M., Stanton, M. L., & Harte, J. (2018). Climate warming drives local extinction:
 964 Evidence from observation and experimentation. *Science Advances*, 4(2), eaaq1819.
 965 <https://doi.org/10.1126/sciadv.aaq1819>
 966 Pascale, S., Boos, W. R., Bordoni, S., Delworth, T. L., Kapnick, S. B., Murakami, H., et al.
 967 (2017). Weakening of the North American monsoon with global warming. *Nature*
 968 *Climate Change*, 7(11), 806–812. <https://doi.org/10.1038/nclimate3412>
 969 Schadt, C. W., Martin, A. P., Lipson, D. A., & Schmidt, S. K. (2003). Seasonal dynamics of
 970 previously unknown fungal lineages in tundra soils. *Science*, 301(5638), 1359–1361.
 971 <https://doi.org/10.1126/science.1086940>
 972 Scherrer, D., & Körner, C. (2011). Topographically controlled thermal-habitat differentiation
 973 buffers alpine plant diversity against climate warming. *Journal of Biogeography*, 38(2),
 974 406–416. <https://doi.org/10.1111/j.1365-2699.2010.02407.x>
 975 Schmidt, S. K., King, A. J., Meier, C. L., Bowman, W. D., Farrer, E. C., Suding, K. N., &
 976 Nemergut, D. R. (2015). Plant–microbe interactions at multiple scales across a high-
 977 elevation landscape. *Plant Ecology & Diversity*, 8(5–6), 703–712.
 978 <https://doi.org/10.1080/17550874.2014.917737>

979 Schuur, E. A. G., McGuire, A. D., Schädel, C., Grosse, G., Harden, J. W., Hayes, D. J., et al.
980 (2015). Climate change and the permafrost carbon feedback. *Nature*, 520(7546), 171–
981 179. <https://doi.org/10.1038/nature14338>

982 Seddon, A. W. R., Macias-Fauria, M., Long, P. R., Benz, D., & Willis, K. J. (2016). Sensitivity
983 of global terrestrial ecosystems to climate variability. *Nature*, 531(7593), 229–232.
984 <https://doi.org/10.1038/nature16986>

985 Spasojevic, M. J., & Suding, K. N. (2012). Inferring community assembly mechanisms from
986 functional diversity patterns: the importance of multiple assembly processes. *Journal of*
987 *Ecology*, 100(3), 652–661. <https://doi.org/10.1111/j.1365-2745.2011.01945.x>

988 Spasojevic, M. J., Bowman, W. D., Humphries, H. C., Seastedt, T. R., & Suding, K. N. (2013).
989 Changes in alpine vegetation over 21 years: Are patterns across a heterogeneous
990 landscape consistent with predictions? *Ecosphere*, 4(9), art117.
991 <https://doi.org/10.1890/ES13-00133.1>

992 Spasojevic, M. J., Harrison, S., Day, H. W., & Southard, R. J. (2014). Above- and belowground
993 biotic interactions facilitate relocation of plants into cooler environments. *Ecology*
994 *Letters*, 17(6), 700–709. <https://doi.org/10.1111/ele.12272>

995 Steinbauer, M. J., Grytnes, J.-A., Jurasinski, G., Kulonen, A., Lenoir, J., Pauli, H., et al. (2018).
996 Accelerated increase in plant species richness on mountain summits is linked to warming.
997 *Nature*, 556(7700), 231–234. <https://doi.org/10.1038/s41586-018-0005-6>

998 Sturm, M., Racine, C., & Tape, K. (2001). Increasing shrub abundance in the Arctic. *Nature*,
999 411(6837), 546–547. <https://doi.org/10.1038/35079180>

1000 Sulman, B. N., Salmon, V. G., Iversen, C. M., Breen, A. L., Yuan, F., & Thornton, P. E. (2021).
1001 Integrating Arctic Plant Functional Types in a Land Surface Model Using Above- and

Belowground Field Observations. *Journal of Advances in Modeling Earth Systems*, 13(4),
e2020MS002396. <https://doi.org/10.1029/2020MS002396>

Swenson, S. C., & Lawrence, D. M. (2014). Assessing a dry surface layer-based soil resistance
parameterization for the Community Land Model using GRACE and FLUXNET-MTE
data. *Journal of Geophysical Research: Atmospheres*, 119(17), 10,299–10,312.
<https://doi.org/10.1002/2014JD022314>

Swenson, Sean C., Clark, M., Fan, Y., Lawrence, D. M., & Perket, J. (2019). Representing
intrahillslope lateral subsurface flow in the Community Land Model. *Journal of
Advances in Modeling Earth Systems*, 11(12), 4044–4065.
<https://doi.org/10.1029/2019MS001833>

Taylor, R. V., & Seastedt, T. R. (1994). Short- and long-term patterns of soil moisture in alpine
tundra. *Arctic and Alpine Research*, 26(1), 14–20. <https://doi.org/10.2307/1551871>

Walker, D., Morse, J., & Niwot Ridge LTER. (2022). *Snow depth data for saddle snowfence,
1992 - ongoing. ver 13*. Environmental Data Initiative. Retrieved from
<https://doi.org/10.6073/pasta/a6a30132f9d4e2d9a0763e7a7faef619>

Walker, M., Smith, J., Humphries, H., & Niwot Ridge LTER. (2022). *Aboveground net primary
productivity data for Saddle grid, 1992 - ongoing. ver 6*. Environmental Data Initiative.
Retrieved from <https://doi.org/10.6073/pasta/b0cdc0cf7c4442f1b2ffc569e9890968>

Walker, M. D., Webber, P. J., Arnold, E. H., & Ebert-May, D. (1994). Effects of interannual
climate variation on aboveground phytomass in alpine vegetation. *Ecology*, 75(2), 393–
408. <https://doi.org/10.2307/1939543>

Walker, M. D., Wahren, C. H., Hollister, R. D., Henry, G. H. R., Ahlquist, L. E., Alatalo, J. M.,
et al. (2006). Plant community responses to experimental warming across the tundra

1025 biome. *Proceedings of the National Academy of Sciences*, 103(5), 1342–1346.

1026 <https://doi.org/10.1073/pnas.0503198103>

1027 Wang, Q., Fan, X., & Wang, M. (2016). Evidence of high-elevation amplification versus Arctic

1028 amplification. *Scientific Reports*, 6(1), 19219. <https://doi.org/10.1038/srep19219>

1029 Wentz, K. F., Neff, J. C., & Suding, K. N. (2019). Leaf temperatures mediate alpine plant

1030 communities' response to a simulated extended summer. *Ecology and Evolution*, 9(3),

1031 1227–1243. <https://doi.org/10.1002/ece3.4816>

1032 Wieder, W. R., Knowles, J. F., Blanken, P. D., Swenson, S. C., & Suding, K. N. (2017).

1033 Ecosystem function in complex mountain terrain: Combining models and long-term

1034 observations to advance process-based understanding. *Journal of Geophysical Research:*

1035 *Biogeosciences*, 122(4), 825–845. <https://doi.org/10.1002/2016JG003704>

1036 Wieder, W. R., Kennedy, D., Lehner, F., Musselman, K. N., Rodgers, K. B., Rosenbloom, N., et

1037 al. (2022). Pervasive alterations to snow-dominated ecosystem functions under climate

1038 change. *Proceedings of the National Academy of Sciences*, 119(30), e2202393119.

1039 <https://doi.org/10.1073/pnas.2202393119>

1040 Wigmore, O., & Niwot Ridge LTER. (2021). *5cm multispectral imagery from UAV campaign at*

1041 *Niwot Ridge, 2017 ver. 1*. Environmental Data Initiative. Retrieved from

1042 <https://doi.org/10.6073/pasta/a4f57c82ad274aa2640e0a79649290ca>

1043 Williams, M. W., Bardsley, T., & Ridders, M. (1998). Overestimation of snow depth and

1044 inorganic nitrogen wetfall using NADP data, Niwot Ridge, Colorado. *Atmospheric*

1045 *Environment*, 32(22), 3827–3833. [https://doi.org/10.1016/S1352-2310\(98\)00009-0](https://doi.org/10.1016/S1352-2310(98)00009-0)

1046 Winkler, D. E., Butz, R. J., Germino, M. J., Reinhardt, K., & Kueppers, L. M. (2018). Snowmelt

1047 Timing Regulates Community Composition, Phenology, and Physiological Performance

1048 of Alpine Plants. *Frontiers in Plant Science*, 9. Retrieved from
 1049 <https://www.frontiersin.org/articles/10.3389/fpls.2018.01140>
 1050 Wookey, P. A., Aerts, R., Bardgett, R. D., Baptist, F., Bråthen, K. A., Cornelissen, J. H. C., et al.
 1051 (2009). Ecosystem feedbacks and cascade processes: understanding their role in the
 1052 responses of Arctic and alpine ecosystems to environmental change. *Global Change*
 1053 *Biology*, 15(5), 1153–1172. <https://doi.org/10.1111/j.1365-2486.2008.01801.x>
 1054 Wutzler, T., Lucas-Moffat, A., Migliavacca, M., Knauer, J., Sickel, K., Šigut, L., et al. (2018).
 1055 Basic and extensible post-processing of eddy covariance flux data with REddyProc.
 1056 *Biogeosciences*, 15(16), 5015–5030. <https://doi.org/10.5194/bg-15-5015-2018>
 1057 Yang, Y., Klein, J. A., Winkler, D. E., Peng, A., Lazarus, B. E., Germino, M. J., et al. (2020).
 1058 Warming of alpine tundra enhances belowground production and shifts community
 1059 towards resource acquisition traits. *Ecosphere*, 11(10), e03270.
 1060 <https://doi.org/10.1002/ecs2.3270>
 1061 Zellweger, F., De Frenne, P., Lenoir, J., Vangansbeke, P., Verheyen, K., Bernhardt-Römermann,
 1062 M., et al. (2020). Forest microclimate dynamics drive plant responses to warming.
 1063 *Science*, 368(6492), 772–775. <https://doi.org/10.1126/science.aba6880>
 1064

Topographic heterogeneity and aspect moderate exposure to climate change across an alpine tundra hillslope

K. R. Jay¹, W. R. Wieder^{1,2}, S. C. Swenson², J. F. Knowles³, S. Elmendorf^{1,4}, H. Holland-Moritz⁵, K. N. Suding^{1,4}

¹Institute of Arctic and Alpine Research, University of Colorado, 4001 Discovery Dr, Boulder, CO 80303, USA.

²National Center for Atmospheric Research, 1850 Table Mesa Dr, Boulder, CO 80305, USA

³Department of Earth and Environmental Sciences, California State University, 400 W. First St, Chico, CA 95929, USA.

⁴Department of Ecology and Evolutionary Biology, University of Colorado, 1900 Pleasant St, Boulder, CO 80302, USA.

⁵Department of Natural Resources and the Environment, University of New Hampshire, 114 James Hall, 56 College Rd, Durham, NH 03824, USA.

Contents of this file

Figures S1 to S4
Table S1

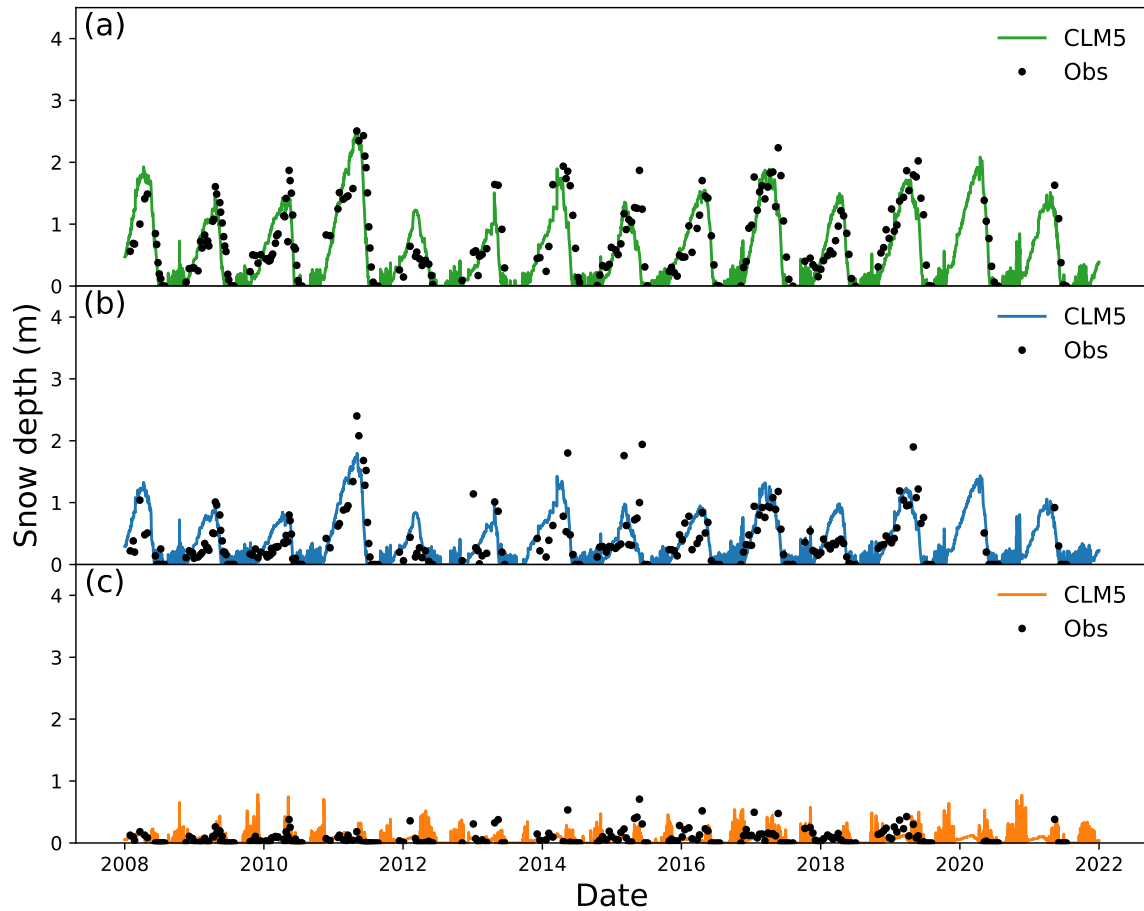


Figure S1. CLM simulations capture the observed variability in the magnitude and timing of snow depth across all three vegetation communities at Niwot Ridge. Time series of observations and CLM simulations from 2008-2021 configured for (a) moist, (b) wet, and (c) dry meadows. Colored lines denote CLM simulations and black points denote ~biweekly snow depth measurements from the Saddle at Niwot Ridge, CO that were averaged by vegetation community and date.

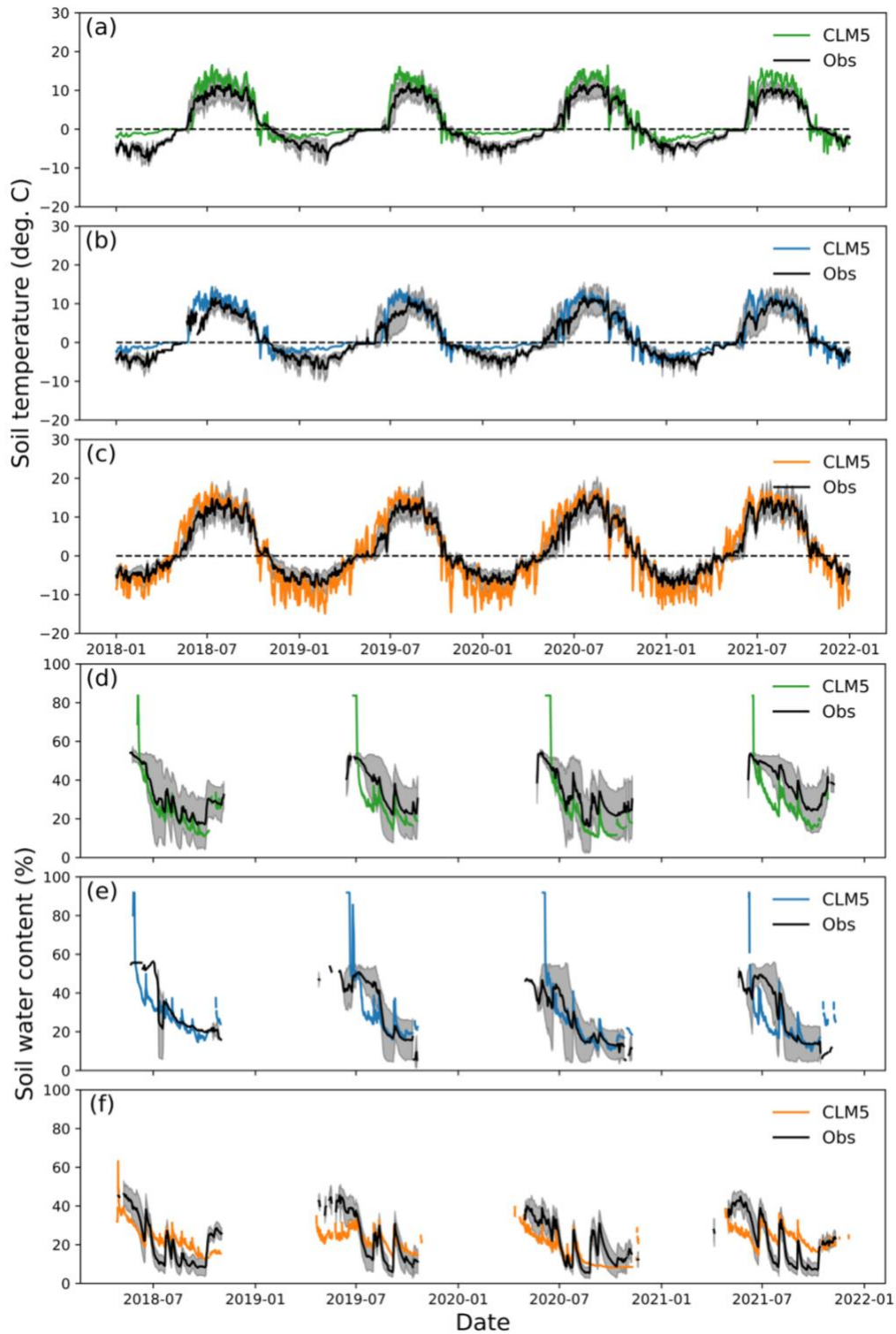


Figure S2. Time series of observations (mean \pm SD) and CLM simulations configured for moist, wet, and dry meadows. (a-c) volumetric soil moisture, and (d-f) soil temperature from 2018-2022 at 5 cm (observations) and 4 cm (CLM simulations) depths. Colored lines denote CLM simulations and black lines denote observations from the sensor network array at Niwot Ridge, CO, where values were averaged across plots for each vegetation community.

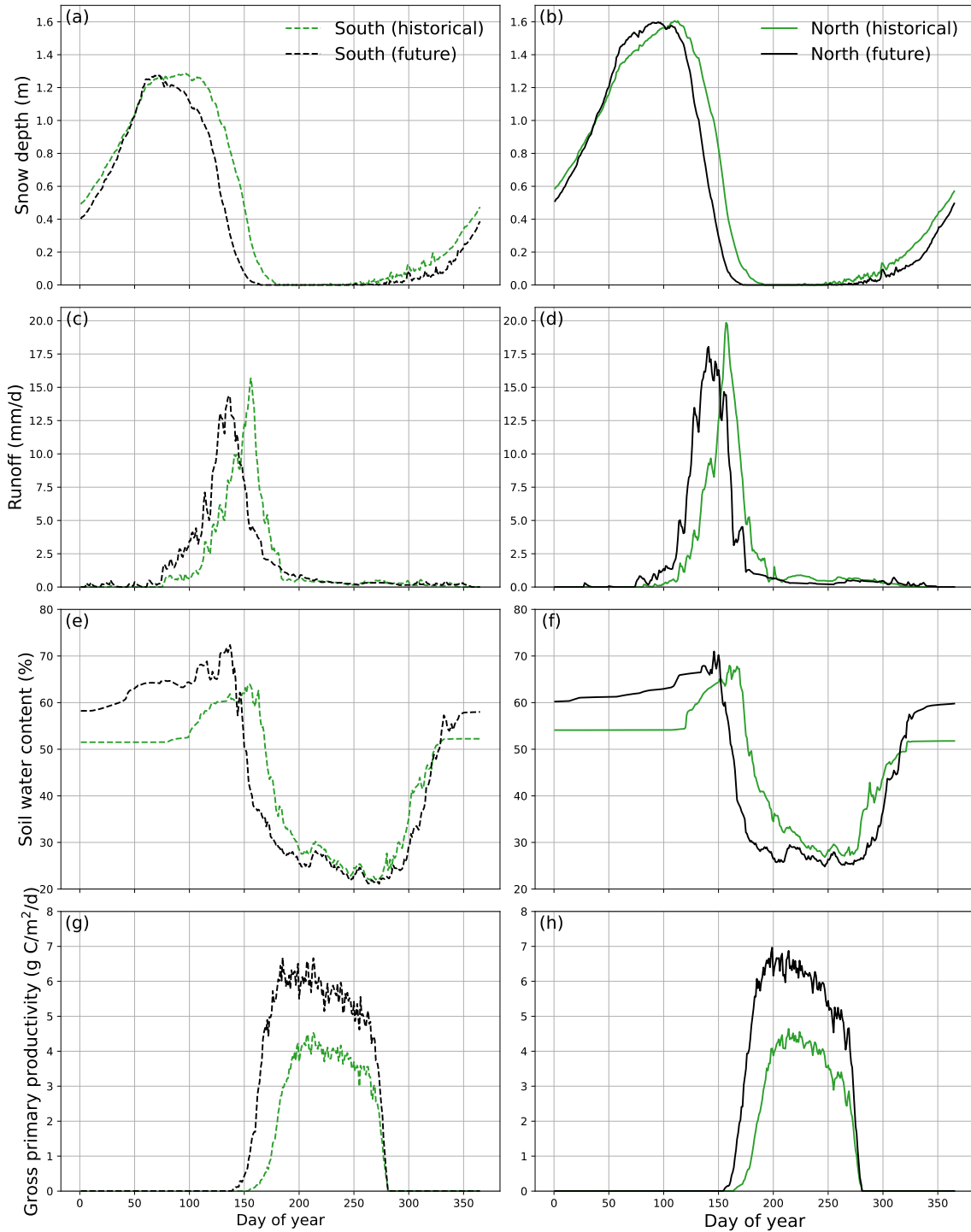


Figure S3. Mean annual climatology of (a, b) snow depth (m), (c, d) runoff (mm/d), (e, f) soil moisture (%), and (g, h) productivity in the moist meadow (upland) column for historical (green lines; 2008-2021) and future (black lines; 2086-2099) time periods. Results from south aspect (dashed lines) are shown in left column and those from north aspect (solid lines) are in right column. Values were averaged by day of year for each time period and aspect. Negative runoff values occur when inflow from uphill is greater than outflow.

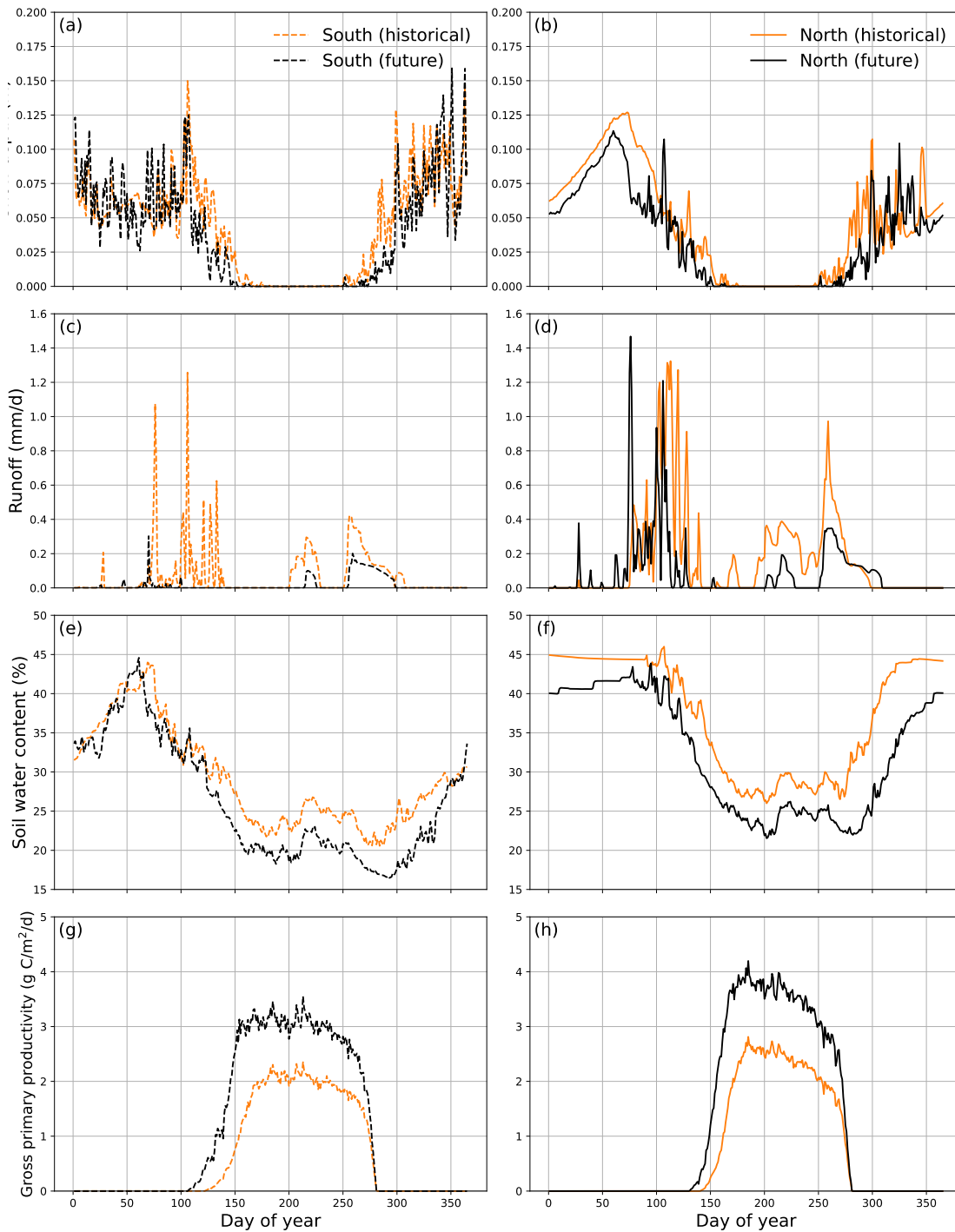


Figure S4. Mean annual climatology of (a, b) snow depth (m), (c, d) runoff (mm/d), (e, f) soil moisture (%), and (g, h) productivity in the dry meadow (upland) column for historical (orange lines; 2008-2021) and future (black lines; 2086-2099) time periods. Results from south aspect (dashed lines) are shown in left column and those from north aspect (solid lines) are in right column. Values were averaged by day of year for each time period and aspect. Negative runoff values occur when inflow from uphill is greater than outflow.

Parameter	Description	Units	Moist Meadow	Wet Meadow	Dry Meadow	Default
<i>slatop</i> ¹	specific leaf area	m ² /gC	0.0215	0.029	0.015	0.0402
<i>leafcn</i> ¹	leaf C:N	gC/gN	19.6	17.7	18.5	28.03
<i>ndays_on</i> ²	# days to complete leaf onset	days	21	28	25	10
<i>crit_onset_gdd_sf</i> ²	scale factor modifying GDD	unitless	1	1	1.7	1
<i>kmax</i>	plant maximum conductance	mm H ₂ O/mm H ₂ O/sec	2.42E-09	2.42E-09	2.30E-10	2.42E-09
<i>krmax</i>	root maximum conductance	mm H ₂ O/mm H ₂ O/sec	8.05E-11	8.05E-11	2.05E-11	8.05E-11
<i>jmaxb₀</i>	baseline proportion of N for electron transport	unitless	0.0225	0.0225	0.0225	0.0331
<i>jmaxb₁</i>	response of electron transport rate to light availability	unitless	0.1	0.1	0.1	0.1745
<i>froot_leaf</i>	new fine root C per new leaf C allocation	gC/gC	1.5	1.5	2	2
<i>d_max</i>	dry surface layer thickness	mm	10	10	10	15
<i>h_bedrock</i>	depth to bedrock	m	1.3	1	1	
<i>wat_sat</i>	water saturation (porosity)	m ³ /m ³			wat_sat/2	
<i>organic</i> ³	organic matter density	kg/ m ³	80.7	107.6	80.7	
<i>sand</i> ³	percent sand	%	49.3	44.4	49.3	
<i>clay</i> ³	percent clay	%	12.7	14	12.7	

¹Values for each vegetation community from Spasojevic et al., (2013).

²Values for each vegetation community derived from Niwot Ridge phenocam green chromatic coordinate (GCC) data set (Elwood et al., 2022) and resulting phenometric calculations (unpublished data)

³Values based on National Ecological Observatory Network (NEON) Megapit (Lombardozzi et al. 2013)

Table S1. Modifications to foliar, hydraulic, and photosynthetic parameters and soil properties to better represent moist, wet, and dry alpine meadow environments. Default values specified in the parameter file are listed for comparison where available. GDD stands for growing degree days.